

Implementation of Iterative Learning Control on a Pneumatic Actuator

by

James Rwafa

Submitted in fulfilment of the academic requirements of

Master of Science

in Electrical Engineering

School of Engineering

College of Agriculture, Engineering and Science

University of KwaZulu-Natal

Durban

South Africa

Supervisor: Dr Farzad Ghayoor

February 2022

PREFACE

The research contained in this dissertation was completed by James Rwafa while based in the Discipline of Electrical Engineering of School of Engineering of the College of Agriculture, Engineering and Science, University of KwaZulu-Natal, Durban, South Africa.

The contents of this work have not been submitted in any form to another university and, except where the work of others is acknowledged in the text, the results reported are due to investigations by the candidate.

Signed: Dr Farzad Ghayoor

Date: ___07/02/2022_____

DECLARATION 1: PLAGIARISM

I, James Rwafa, declare that:

- (i) the research reported in this dissertation, except where otherwise indicated or acknowledged, is my original work;
- (ii) this dissertation has not been submitted in full or in part for any degree or examination to any other university;
- (iii) this dissertation does not contain other persons' data, pictures, graphs or other information, unless specifically acknowledged as being sourced from other persons;
- (iv) this dissertation does not contain other persons' writing, unless specifically acknowledged as being sourced from other researchers. Where other written sources have been quoted, then:
 - a) their words have been re-written but the general information attributed to them has been referenced;
 - b) where their exact words have been used, their writing has been placed inside quotation marks, and referenced;
- (v) where I have used material for which publications followed, I have indicated in detail my role in the work;
- (vi) this dissertation is primarily a collection of material, prepared by myself, published as journal articles or presented as a poster and oral presentations at conferences. In some cases, additional material has been included;
- (vii) this dissertation does not contain text, graphics or tables copied and pasted from the Internet, unless specifically acknowledged, and the source being detailed in the dissertation and in the References sections.



Signed: James Rwafa

Date: 07/02/2022

DECLARATION 2: PUBLICATIONS

DETAILS OF CONTRIBUTION TO PUBLICATIONS that form part and/or include research presented in this dissertation:

Publication 1:

Rwafa, J., and F. Ghayoor. "Implementation of Iterative Learning Control On A Pneumatic Control Valve." in *2019 International Multidisciplinary Information Technology and Engineering Conference (IMITEC)*, pp. 1-5. IEEE, 2019. (*IMITEC 2019*). Vanderbijlpark, South Africa, South Africa

The papers were authored by James Rwafa and co-authored by Farzad Ghayoor.



Signed: James Rwafa

Date: 07/02/2022

ABSTRACT

Pneumatic systems play a pivotal role in many industrial applications, such as in petrochemical industries, steel manufacturing, car manufacturing and food industries. Besides industrial applications, pneumatic systems have also been used in many robotic systems. Nevertheless, a pneumatic system contains different nonlinear and uncertain behaviour due to gas compression, gas leakage, attenuation of the air in pipes and frictional forces in mechanical parts, which increase the system's dynamic orders. Therefore, modelling a pneumatic system tends to be complicated and challenges the design of the controller for such a system. As a result, employing an effective control mechanism to precisely control a pneumatic system for achieving the required performance is essential.

A desirable controller for a pneumatic system should be capable of learning the dynamics of the system and adjusting the control signal accordingly. In this study, a learning control scheme to overcome the highlighted nonlinearity problems is suggested. Many industrial processes are repetitive, and it is reasonable to make use of previously acquired data to improve a controller's convergence and robustness. An Iterative Learning Control (ILC) algorithm uses information from previous repetitions to learn about the system's dynamics. The ILC algorithm characteristics are beneficial in real-time control given its short time requirements for responding to input changes.

Cylinder-piston actuators are the most common pneumatic systems, which translate the air pressure force into a linear mechanical motion. In industrial automation and robotics, linear pneumatic actuators have a wide range of applications, from load positioning to pneumatic muscles in robots. Therefore, the aim of this research is to study the performance of ILC techniques in position control of the rod in a pneumatic position-cylinder system. Based on theoretical analysis, the design of an ILC is discussed, showing that the controller can satisfactorily overcome nonlinearities and uncertainties in the system without needing any prior knowledge of the system's model. The controller has been designed in such a way to even work on non-iterative processes. The performance of the ILC-controlled system is compared with a well-tuned PID controller, showing a faster and more accurate response.

ACKNOWLEDGMENTS

My sincere gratitude goes to my supervisor, Dr Farzad Ghayoor, for his unwavering support, knowhow and mentoring. Sometimes there are times when one wants to give up, but he motivated me through and through to an extent that I cannot stop studying. Secondly, I would like to thank the UKZN Electrical Postgraduate staff for their assistance in the logistics that are required in order to enrol for postgraduate studies. Lastly, there is the social life that runs parallel with the academic life. I dedicate this dissertation to my lovely wife Joyce Rwafa. She gave me love and support and always looked forward for another day because of her nurturing.

TABLE OF CONTENTS

PREFACE ii

DECLARATION 1: PLAGIARISM..... iii

DECLARATION 2: PUBLICATIONS iv

ABSTRACT v

ACKNOWLEDGMENTS..... vi

TABLE OF CONTENTS vii

LIST OF TABLES ix

LIST OF FIGURES..... x

CHAPTER 1: INTRODUCTION 1

 1.1. Background 1

 1.2. Motivation 1

 1.2.1. General Motivation for the Study 1

 1.2.2. Motivation for the Adopted Approach..... 2

 1.3. Problem Statement 3

 1.4. Aims and Objectives 3

 1.5. Outline of Dissertation Structure..... 4

CHAPTER 2: LITERATURE REVIEW 5

 2.1. Introduction 5

 2.2. Methods of Controlling a Pneumatic Actuator 6

 2.2.1. Controlling Based on PID Controllers..... 6

 2.2.2. Controlling Based on Robust Controllers..... 8

 2.2.3. Controlling Based on Adaptive Controllers 9

 2.2.4. Controlling Based on Intelligent Controllers..... 9

 2.3. Iterative Learning Controller..... 10

 2.4. Summary 12

CHAPTER 3: MATHEMATICAL MODELLING AND SIMULATION..... 14

 3.1. Introduction 14

 3.2. Supply unit 15

3.3. The Pipe Model	18
3.4. The Valve Model.....	21
3.5. The Cylinder Model	24
3.6. The Simulation of the Pneumatic System	27
3.7. Summary	35
CHAPTER 4: ITERATIVE LEARNING CONTROLLER DESIGN	36
4.1. Introduction	36
4.2. PID Controller Design for the Pneumatic Actuator	36
4.3. Iterative Learning Control Techniques	39
4.4. Controller Design	42
4.5. Summary	53
CHAPTER 5: CONCLUSION.....	55
References	58

LIST OF TABLES

Table 3.1. Parameters values used in simulation 27

LIST OF FIGURES

Figure 3.1. The pneumatic actuator.....	15
Figure 3.2. The Simscape model of the supply unit.....	17
Figure 3.3. The Simscape model of the pipe.....	21
Figure 3.4. The Simscape model of the valve.....	23
Figure 3.5. The Simscape model of the cylinder.....	26
Figure 3.6. The gas property plot for dry air considered in the simulation.....	29
Figure 3.7. Effect of the valve's input voltage on the rod's displacement.....	30
Figure 3.8. Pressure drop and temperature difference across the supply pipe (P).....	30
Figure 3.9. Pressure drop and temperature difference across the exhaust pipe (T).....	31
Figure 3.10. Pressure drop and temperature difference across pipe (A).....	31
Figure 3.11. Pressure drop and temperature difference across pipe (B).....	32
Figure 3.12. Changes in the input valve cross-sectional area with the applied voltage.....	32
Figure 3.13. Mass flow rate in the valve versus the applied voltage.....	33
Figure 3.14. Changes of pressure, temperature and volume in Chamber 1.....	33
Figure 3.15. Changes of pressure, temperature and volume in Chamber 2.....	34
Figure 3.16. The pneumatic system estimated frequency response.....	35
Figure 4.1. Nichols Chart of the plant.....	36
Figure 4.2. Nichols chart of the PID controlled actuator.....	37
Figure 4.3. Tracking performance of the PID controlled actuator.....	38
Figure 4.4. Tracking error for the PID controlled actuator.....	38

Figure 4.5. Inverse Nichols chart of the PID controlled actuator	39
Figure 4.6. Performance of the PID controlled actuator under payload uncertainty	39
Figure 4.7. ILC Architecture	40
Figure 4.8. Example of an ILC structure.....	42
Figure 4.9. The effect of learning function value on the σ	50
Figure 4.10. Tracking performance of the ILC controlled actuator	51
Figure 4.11. The comparison between the ILC and PID performance in tracking a reference signal	51
Figure 4.12. Comparison of PID and ILC with respect to the tracking error.....	52
Figure 4.13. Performance of the ILC controlled actuator under payload uncertainty	53
Figure 4.14. Comparison of PID and ILC with respect to overcoming payload uncertainty...	53

CHAPTER 1: INTRODUCTION

1.1. Background

In industrial processes, it is common to adjust fluid flow rates or machinery' positions and speeds to meet specific requirements for achieving certain outcomes. For example, through throttling a fluid flow, a certain flow rate, speed, composition or density can be achieved. Many types of machinery in manufacturing processes are required to be accurately positioned. The movement can be made possible by the use of actuators. The actuator mechanism can be manual, hydraulic, pneumatic or electromechanical.

Pneumatic actuators have some advantages over their hydraulic and electromechanical counterparts. Unlike hydraulic systems, no temperature limitation is imposed on pneumatic systems. The pneumatic systems use air, which allows the exhaust gases to be released into the atmosphere, and eliminates the need for the return pipes in the system. Moreover, a pneumatic system can be easily stored for a long time as it is virtually dry. Compared to electromechanical systems, pneumatic systems generate a higher power density over a greater operation bandwidth without causing any electromagnetic interferences.

Jackhammers, pneumatic cylinders, pneumatic boosters, power drills and direction control valves are examples of widely used pneumatic systems. Generally, pneumatic systems are cheaper, safer, cleaner, and easier to maintain [1]. In many manufacturing processes, such as steel and car manufacturing, pneumatic systems have been extensively used, and in fact, they play a pivotal role in the petrochemical and food industries.

1.2. Motivation

1.2.1. General Motivation for the Study

Pneumatic systems use the force generated by compressed air in their operation. The air is, however, compressible and has a low damping characteristic, which causes a nonlinear response and increases the system's dynamic order. Moreover, before the system can apply any force to a load, a pneumatic system's pipes and cylinders have to be filled with air. This results in further

nonlinearities in the form of dead-band and transmission attenuations. Also, a pneumatic system is affected by frictional forces caused by the mechanical parts' movements. Such uncertainties and nonlinearities in a pneumatic system make its modelling a complicated practice. This might have negative effects on the precise control of the system, depending on the selected control algorithm. Therefore, there would be a need for a control approach capable of overcoming the mentioned challenges.

The most commonly used controllers in industrial applications are Programmable Logic Controllers (PLCs), which, as their name suggests, use logical signals to control a system. However, due to the nonlinear nature of pneumatic systems, PLCs cannot achieve the desired performance in controlling a pneumatic system. Employing Proportional-Integral-Derivative (PID) controllers is another conventional method in controlling industrial processes. Nevertheless, PID controllers experience gain tuning problems in systems with nonlinearities and uncertainties. The PID controllers are used in conjunction with adaptive and intelligent controllers to obtain the desired level of performance in pneumatic systems. Robust controllers have also been utilized in controlling pneumatic actuator systems to overcome uncertainties. The ability to adapt to the system's variation is the common characteristic held by the most successful algorithms used in controlling pneumatic systems [2].

1.2.2. Motivation for the Adopted Approach

A controller should enable a system to accurately track a reference signal over a period of time despite potential variations in the system. In many control algorithms, the model of the system has to be achieved prior to the design of the controller. However, due to the gases' physical behaviour, modelling a pneumatic system is usually done based on many assumptions that might result in an inaccurate model during the system operation. As a result, such controllers may not achieve the required performance. This leads to developing real-time control systems capable of controlling pneumatic systems without needing to obtain the mathematical model of the system.

An Iterative Learning Control (ILC) algorithm uses information from previous repetitions to learn about the system's dynamics for generating a more suitable control signal. This learning process is performed in an iterative manner to improve the controller's performance from one

iteration to the other, achieving a zero-error convergence. ILC algorithms are particularly useful in real-time control systems, given their relatively quick response to the changes of the input signal.

Many industrial processes are repetitive, which means the same control action should be performed repeatedly. Therefore, it is reasonable to make use of previously acquired data for improving a controller's convergence and robustness in such processes. In this study, an ILC method will be suggested to overcome the nonlinearities and uncertainties resulting from air characteristics, pressure loss, leakage and load variations in a pneumatic system. This control algorithm should be capable of adapting to the system's dynamics and adjusting the control signal accordingly.

1.3. Problem Statement

The position control of a pneumatic piston-cylinder system affected by a variety of factors and disturbances is considered in this research. In addition to the nonlinearities and uncertainties resulting from the physical characteristics of the air, the dynamics of a cylinder and the friction losses in the pneumatic servo system are considered. An ILC algorithm is designed to precisely control the position of the rod in a pneumatic piston-cylinder system. The ILC method learns the system's behaviour from the system's input and output and tries to achieve the required performance through minimizing error with multiple iterations. Therefore, no prior knowledge of the system model is required.

1.4. Aims and Objectives

The aim of this research is to design an ILC controller for position control of a pneumatic system to achieve a certain level of performance. As a result, the following objectives have to be achieved:

- 1) To model and simulate a pneumatic piston-cylinder system by considering the nonlinearities and uncertainties affecting the system.

- 2) To design and employ ILC techniques to control the position of the rod of the modelled pneumatic piston-cylinder system. The system should converge to steady-state conditions within a minimum allowable time and be robust against uncertainties. For this purpose, the control system measures the system's errors and learns from the recurrence and accumulation of these errors to develop a control algorithm for achieving stability through eliminating the errors.
- 3) To compare the performance of the ILC to a conventional controller such as a well-tuned PID controller.

1.5. Outline of Dissertation Structure

The rest of this dissertation is outlined as follows:

Chapter 1 covered the background and motivation of the study. This was followed by the motivation for selecting the adopted approach, the problem statement and the objectives of this research. Chapter 2 presents an overview of the literature on controlling pneumatic systems and different ILC techniques. In Chapter 3, the mathematical model and simulation of the selected pneumatic system are discussed. The controller design for the selected pneumatic system is covered in Chapter 4, and the performance of the system has been investigated. Finally, the research is concluded in Chapter 5.

CHAPTER 2: LITERATURE REVIEW

2.1. Introduction

In pneumatic actuators, the energy of compressed air is converted into mechanical force, causing rotary or linear motions. Cylinder-piston actuators are the most common types of pneumatic systems, which translate air pressure energy into a linear motion. Linear pneumatic actuators have a wide range of applications in industrial automation and robotics, from load positioning [3] to active suspension of vehicles [4], heavy-duty vehicles' air-brake systems [5], conveyor belt systems [6, 7] and pneumatic actuator muscle (PAM) [8-10] of robots.

Nevertheless, there are limitations in employing pneumatic actuators in applications that require high stability, precision and robustness. These limitations are due to the existence of different nonlinear behaviours caused by dead-zone, air compressibility, friction and airflow rate parameters in pneumatic systems [11-14]. Such nonlinearities make identifying pneumatic systems' parameters, which are needed by many control algorithms to precisely control the system's position, a challenging practice.

The development of controllers for pneumatic servo systems began in the 1990s and has continued to expand in recent years. The most commonly used controller in industrial applications is the PID controller. This traditional type of controller is used in conjunction with other controllers, including intelligent controllers, to obtain the desired level of performance in pneumatic systems. Other nonlinear and adaptive control techniques have also been utilized in controlling pneumatic actuator systems.

The aim of this research is to design an ILC controller for position control of a pneumatic system. Therefore, in this chapter, first, a literature review on the methods of controlling pneumatic actuators is provided. Several studies have been explored to find ways of controlling pneumatic servo systems and overcome challenges. This follows by covering the work done on designing iterative learning controllers.

2.2. Methods of Controlling a Pneumatic Actuator

Early work on controlling pneumatic actuators using microprocessors was theoretically based on linearizing pneumatic models [15]. Moreover, techniques such as increasing the number of feedback loops were used to improve the transient response of pneumatic servo drives [16]. It was shown in [17] that achieving a control method capable of withstanding payload fluctuations requires an accurate model of the actuator and sufficient output measurement. These requirements are usually difficult to obtain using a single feedback loop. However, a desired level of robustness can be achieved by getting feedback signals from both force and velocity outputs [18]. Moreover, a loop shaping method was considered in [19] to reduce the effects of vibration without taking into account the impacts of external uncertainties on the system's performance.

2.2.1. Controlling Based on PID Controllers

The design of controllers for pneumatic systems began during the 1990s by proposing different PID methods. As an early attempt, a conventional PID controller was combined with a friction compensator to generate a pulse width modulation (PWM) signal for controlling an on/off solenoid valve in a pneumatic cylinder-piston system [3]. This controller could position the piston's rod regardless of uncertainties in the payload but could not sufficiently reduce rise-time and steady-state error. To improve position controlling, a modified PID controller is suggested in [20] for pneumatic actuators that are used in the food packaging industry. PID controllers have been combined with velocity feedforward and feedback compensators to overcome friction [21] and are combined with acceleration feedback to improve response accuracy. The combination of PID controllers with acceleration feedback and nonlinear compensators could improve the level of accuracy in position control of a pneumatic system [22]. A PD feedback controller with saturation was designed based on linearized mathematical models and showed that it would be capable of tracking a large class of reference trajectories [23].

The Ziegler-Nichols method's effectiveness in adjusting parameters of a conventional PID controller for controlling the position of a pneumatic actuator has been studied [24, 25]. It was shown that the system could not be controlled with only a proportional controller as the

system's output would oscillate around the setpoint. Despite the unsatisfactory performance of PI controllers in controlling the system, PD compensators were able to eliminate oscillations and improve the rise-time. The steady-state error and the response rise-time were further reduced when the system was controlled by a well-tuned PID controller. However, this was at the price of increasing the response's overshoot.

Even though it was shown in [24] that a conventional PI compensator could not control pneumatic actuators, [26] proposed an approach for designing PI controllers capable of obtaining precise position control. For this purpose, a self-tuning method for adjusting the PI controller was proposed, where the placement of the pole was adapted according to the system's parameters and payload. Compared to a conventional PI controller, the self-tuning pole-placement technique had a faster transient response, higher stability, and a lesser steady-state error. A pole-placement controller has also been combined with a dead-zone compensator to further improve the performance of the controller [27].

Two PID control loops have been used in [28] to control the position of a pneumatic system. The inner loop used a feedback PID controller for controlling the pressure, while the outer loop employed a PID controller to compensate for the friction and control the position. The performance of cascaded PID controllers that were tuned by the particle swarm optimization (PSO) method was studied in [29]. The model of the pneumatic system was better identified by the PSO, and so the obtained PID showed improved performance in controlling both the speed and position of pneumatic actuators. The study showed that cascaded PID controllers tuned with PSO would outperform a single PID controller with respect to obtaining a faster response and lesser steady-state errors. PSO is not the only optimization method that has been used for tuning controllers. The genetic algorithm has also been used in [30, 31] to optimise PID controller parameters used in position controlling of a pneumatic servo system.

Although conventional linear PID controllers are the primary options in many industrial applications, they cannot satisfy the desired level of robustness, accuracy and response time in controlling pneumatic systems. This is mainly due to the nonlinear dynamics of pneumatic systems. Designing PID controllers for nonlinear systems was discussed in [32]. For regulating the position of a pneumatic actuator, nonlinear-PID (NPID) controllers were designed in [33, 34] and combined with a dead-zone compensator [35]. The range and rate variations are the

two parameters that have to be specified in designing an NPID controller. Self-regulated NPID (SN-PID) controllers can automatically adjust these parameters and improve the performance of the NPID. [36] combined an SN-PID with a multi-nonlinear-PID (MN-PID) controller to control a pneumatic system, where the fuzzy logic was utilized to adjust the rate variation component of MN-PID.

2.2.2. Controlling Based on Robust Controllers

The robust controller consists of techniques to deal with bounded uncertainties in a loop. In many robust controller designs for pneumatic systems, first, the system was linearized using feedback linearization approaches, and then robust control methods, such as the H_∞ , were applied to the system [37-39]. Quantitative feedback theory (QFT) is the other robust control approach that has been used in controlling pneumatic systems. In [40, 41], QFT controllers were designed to control a pneumatic system under variable payload while satisfying the required tracking and stability constraints.

The most widely used robust controller design for pneumatic systems is based on the sliding mode control (SMC) theory, which is a nonlinear control method. The first designed SMC method for position control of a pneumatic cylinder was presented in [42] and showed great tracking performance under payload fluctuation for second-order pneumatic servo systems. The dynamics of the system and Lyapunov stability theory were considered in designing the controller. Full order and reduced order SMC controllers were used in [43] to control force in a pneumatic servo system, concluding that a full order SMC is the recommended method for high accuracy and speed applications. SMC theory has been applied to different orders of pneumatic cylinder actuators to track the piston position [44, 45]. To enhance the performance of the SMC controller, [46] suggested a multiple-surface SMC controller, and [47] considered a seven-mode sliding controller. A method to reduce the chattering effect in SMC controllers was proposed in [48]. SMC controllers can also be combined with linear controllers, as in [49], where PI and SMC controllers were combined to reduce the impact of valve friction in a pneumatic system. Although based on SMC theory, an efficient controller for a pneumatic actuator, which contains an imprecise, high-order, nonlinear dynamic model, can be obtained, the SMC controller action causes chattering due to its switching nature.

2.2.3. Controlling Based on Adaptive Controllers

Adaptive control can also deal with the plant's variations. However, as opposed to the SMC theory, no prior information on uncertainties' boundaries is required. In adaptive control techniques, the controller estimates the system's parameters using measurements and adapts itself to the changes, which would occur in the system. In [50], the function approximation method is used for designing an adaptive controller for pneumatic systems. The assumed models contained nonlinearities and uncertainties, and operated under disturbances from the applied payload. [51] used the Lyapunov function approach to develop a unique adaptive sliding mode control rule. A model reference adaptive controller is designed in [52] to overcome friction and payload fluctuations in a pneumatic actuator. In [53], an adaptive back-stepping method is used with a PID controller to control a robotic hand.

The adaptive control has also been combined with intelligent control to achieve better performance. [54, 55] proposed adaptive neuro-fuzzy controllers for controlling the position of pneumatic servo systems. Recently, the focus has been shifted towards nonlinear characteristic elimination without modelling the systems. As a result, intelligent adaptive control methods are currently more trending.

2.2.4. Controlling Based on Intelligent Controllers

Fuzzy logic and neural network-based controllers have been extensively used in robotic applications, and they both have shown great potential in controlling complex, time-varying, nonlinear systems. However, the computational complexity of these types of controllers is usually high and requires powerful processing units. Fuzzy controllers were used for controlling servo pneumatic systems [56-58] and PAM [10] and have shown satisfactory performance. Saravanakumar et al. [59, 60] showed that Fuzzy controllers outperform ordinary PID compensators. Using neural networks in controlling a single-rod pneumatic manipulator was studied in [61, 62] and showed it could obtain strong robustness and satisfactory performance. The learning vector quantization neural network method was used as a switching algorithm in controlling two PAM manipulators [63]. The combination of Fuzzy logic and neural networks, which is known as a fuzzy-neural network (FNN) controller, was also tested in controlling

pneumatic systems [64] and PAM manipulators [65]. Extended Kalman filter and back-propagation algorithms were used in developing FNN algorithms.

Another approach for using intelligent controllers in a control loop is by combining them with other conventional controllers. The intelligent controllers are used to tune the conventional controllers' parameters, and thus the designed controllers can be used in different types of pneumatic actuators. In [66, 67], combinations of fuzzy logic and PD controllers were proposed for pneumatic positioning systems, and the controlled systems demonstrated stability and disturbance rejection capability. The PI and fuzzy controllers were also combined in [68] for position control of a pneumatic actuator. Self-tuning fuzzy-PID regulators for controlling pneumatic servo systems were suggested in [69, 70], and designing cascaded self-tuning fuzzy PID controllers for both position and pressure control was covered in [71]. Neural networks were also used in tuning PID [72] and NPID [8] controllers for controlling pneumatic actuators.

The ILC has also been classified as an intelligent control method. [73] employed ILC for controlling a pneumatic actuated X-Y table, and [74] used ILC with PID to control a simplified model pneumatic servo system. Recently, the ILC method was proposed for accurate tracking of PAM [75, 76] and pneumatic valves [77]. The next section provides a literature review on ILC techniques.

2.3. Iterative Learning Controller

ILC term was first used in [78] to describe a control method capable of learning from its experience in controlling a plant. Nevertheless, the idea of iterative learning control was patented in 1971 [79] as "Learning control of actuators in control systems" and was published in the Japanese language in 1978 [80]. The difference between ILC and other learning-type control methods, such as intelligent control and adaptive control, is that the ILC only modifies the control signal according to a predefined control law. However, other learning-type controllers update their control laws during the process by monitoring the system's performance [81]. Unlike an adaptive controller, which requires accurate modelling of the system, the ILC method almost does not need any information on the system model, and it only operates based on the system's historical input and output. Also, contrasting to intelligent controllers, no

training is required, and a well-selected ILC method should be able to converge to the expected state with a few iterations [82].

The objective of the ILC is to improve control action through repetition. The control signal in every iteration is calculated using the input and output information from previous repetitions such that the error decreases in every iteration and eventually becomes zero [83]. In this way, the ILC method is similar to the repetitive control (RC) methods [84]. However, the assumption in the ILC method is that all iterations start at the same initial condition, whereas in the RC method, the final state of the existing repetition would be the initial state for the next one. This difference led to different analysis techniques and results [85].

The ILC is a feedforward method capable of improving the tracking performance and transient response of uncertain time-variant systems that repeatedly run over a fixed period of time. It is also capable of overcoming external disturbances and uncertainties within the system. Therefore, it is considered a suitable method for controlling systems that perform repetitive tasks [86]. The ability of the ILC to anticipate and respond in advance to repetitive disturbances is one of the advantages that it has over traditional feedforward and feedback controllers. However, the pre-emptive ability of ILC depends on the causality of the learning algorithm. Despite the concept of non-causality, a non-causal control system is easily feasible in the ILC as the entirety of the time sequence data is attainable from previous iterations.

Since causality has implications for feedback equivalence, converged control in ILC can be obtained by the way of a feedback controller [87-89]. In a noise-free scenario, [88] shows that there is a feedback equivalence for casual ILC algorithms and that an equivalent feedback controller can be achieved directly from the learning algorithm. This essentially means that causal ILC algorithms are of little significance as the same control action can be provided by a feedback controller without the learning process. However, causal algorithms should not be disregarded for this reason. There are vital restrictions to the equivalent feedback controller, which rationalises and defends the use of causal ILC algorithms. To justify why causal ILC algorithms should continue to be in use, as aforementioned in [88], feedback control equivalence is restricted to noise-free scenarios. The increase in ILC performance means that the equivalent feedback controller has an increasing gain [88]. This in return affects the performance, degrades equipment and leads to instability [89]. Considering all the above-

mentioned points, causal algorithms are still important in practical implementation and are of great value.

An ILC algorithm was initially modelled in continuous form but considering that it requires the storage of previous iteration data, discrete-time is the most suitable domain for implementing an ILC method [90-92]. ILC's learning algorithms can be defined as linear time-invariant and linear time-varying, nonlinear and iteration-varying functions [81, 93-96]. Chen and Wen [97] proposed a high-order ILC (HOILC), where a control law was defined based on a finite number of previous trials. This idea has been further developed in [96, 98-100]. It is shown that by including the existing iteration into the learning algorithm, the ILC can also cover a conventional feedback control algorithm [101].

The ILC design based on discrete-time linearization of nonlinear systems showed acceptable performance in controlling nonlinear systems [92, 93, 102-105]. Both linear and nonlinear learning algorithms have been considered for controlling nonlinear systems. The linear ILC has been developed for global Lipschitz continuous (GLC) systems and the nonlinear ILC for local Lipschitz continuous (LLC) systems. In GLC systems, the control objective is output tracking, and it is expected that only output information is accessible. In LLC systems, the control objective is state tracking, so the state information must be accessible. Analysis of ILC showed that the linear ILC law below can guarantee a geometric convergence despite the system's nonlinearities and indefinite dynamics [78, 106].

The ILC has also been considered for non-repetitive processes and has shown its applicability in controlling such systems [107, 108]. An initial state learning mechanism is suggested in [109] to function between two successive iterations. As a result, this places the initial state at a designated place and converges asymptotically.

2.4. Summary

In this chapter, first, the methods of controlling pneumatic actuators were reviewed, where they were classified into PID-based, robust methods, adaptive methods and intelligent based controllers. It was discussed that the main challenge in controlling pneumatic actuators is to overcome the nonlinearities and uncertainties of the system. Two approaches have been taken

for designing controllers for pneumatic systems. In the first approach, as is done in robust control methods, uncertainty boundaries are identified and the controller is designed within those boundaries. In the second approach, the controllers are capable of being adjusted to the system's variations. However, this requires continuously estimating the system's parameters using measurements, as is done in adaptive controllers, or performing extensive calculations and training as in intelligent based methods. A well-tuned PID controller can also achieve the required performance. The tuning can be done by the designer or by the system itself using different adaptive and intelligent methods. The ILC, which is classified as an intelligent controller, is a control approach that uses the historical information of the system's inputs and outputs to produce a control signal. The method is model-free and has the potential to be used for controlling nonlinear systems. Therefore, in the final section of this chapter, the work done on the ILC methods has been reviewed.

CHAPTER 3: MATHEMATICAL MODELLING AND SIMULATION

3.1. Introduction

In order to have a better understanding of the nonlinearities and uncertainties in a pneumatic system, this chapter discusses the mathematical model and physical properties of a pneumatic actuator. Pneumatic actuators can be modelled based on several approaches. In the most widely used approach, a pneumatic actuator is modelled according to theoretical analysis, including thermodynamics, fluid mechanics and motion dynamics theories. Modelling a pneumatic system consists of identifying:

- 1) Mass and heat flow rates in the system,
- 2) Pressure drops across valves and pipes; and
- 3) Dynamics of the mechanical motions.

In addition to the mathematical model derivation, this chapter covers the simulation of the system using MATLAB SimScape, which enables the accurate modelling of the physical systems within the Simulink environment. The required pneumatic and mechanical subsystems are modelled by assembling the fundamental components and using physical connections.

The pneumatic actuator that will be used in this research is in the form of a double-acting pneumatic cylinder controlled by a 4-port-3-position (4/3) electro-pneumatic valve, as is depicted in Figure 3.1. The piston's rod in this system is connected to an external load, and its position is monitored by a position sensor. A 4/3 valve comprises four ports and three distinctive states. The valve consists of the inlet (P) and exhaust (T) ports and the two ports, depicted as ports A and B, connecting to the chambers of a cylinder. The considered valve is a close-centre, which means when the valve is at its neutral position (middle state), all ports will be closed. When the valve moves to its left-hand side state, the air flows into port A and exhausts from port B; and when it is at the right-hand side state, the air flows into port B and exhausts from port A. A positive applied voltage to port S takes the valve to its left-hand side state, and a negative voltage changes the valve state to its right-hand side. Therefore, a positive applied voltage would push the load away from the cylinder, while a negative voltage would drag the load towards the cylinder.

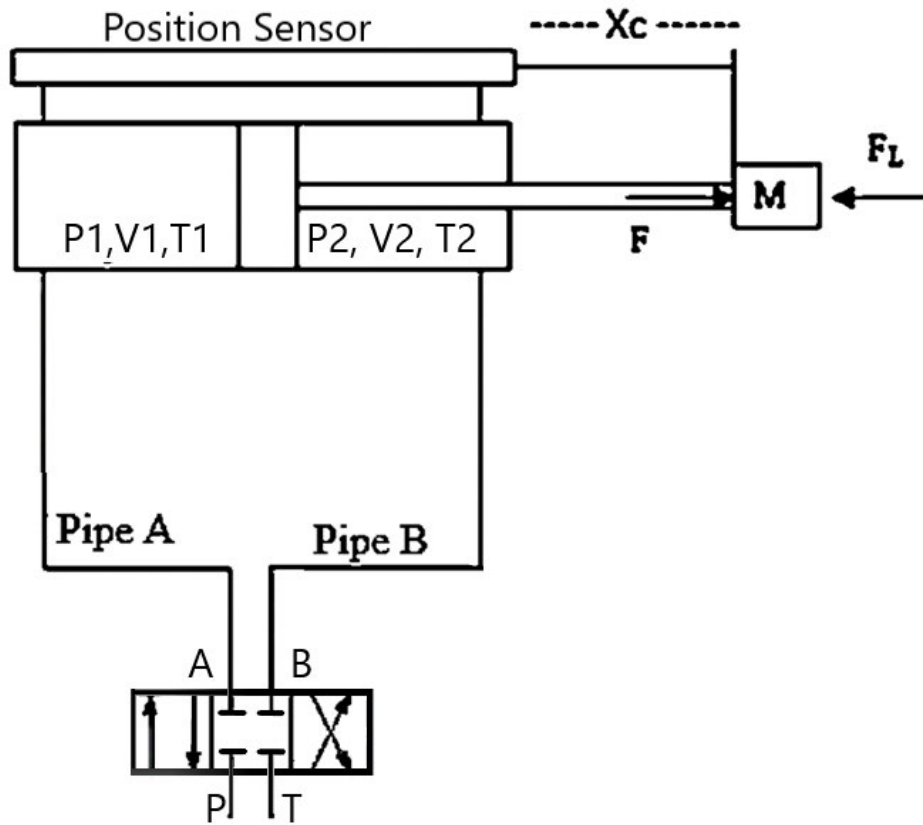


Figure 3.1. The pneumatic actuator

3.2. Supply unit

The ideal gas law has been considered in modelling the pneumatic actuator. According to this law

$$P = z\rho RT \quad (3-1)$$

where P, ρ, z and T are the gas's pressure, density, compressibility factor and temperature, respectively, and R is the gas constant. The perfect gas is sufficiently accurate for modelling dry air at standard conditions [43]. The specific enthalpy, h , for an ideal gas is calculated as

$$h = u + Pv \quad (3-2)$$

where u and v are the internal energy and volume per unit mass of the gas. Under constant pressure, the change in specific enthalpy with respect to temperature, known as the specific heat capacity, is equal to

$$C_p = \left(\frac{\partial h}{\partial T} \right)_p \quad (3-3)$$

and similarly, the change in specific enthalpy with respect to temperature under constant volume is equal to

$$C_v = \left(\frac{\partial h}{\partial T} \right)_v \quad (3-4)$$

The ratio of the heat capacities is equal to

$$\gamma = \frac{C_p}{C_v} \quad (3-5)$$

which is called the specific heat ratio. The above properties, together with the thermal conductivity and dynamic viscosity, which will be used in modelling the gas transport behaviour, are defined in the Simscape Gas properties block.

The system's reference temperature and pressure, which are taken as atmospheric temperature and pressure in this model, are defined in the Reservoir block of the Simscape. The reservoir is assumed to be an infinite volume of gas capable of maintaining a constant temperature and pressure. The reservoir's outflow stream has the same pressure and temperature as the gas inside the reservoir. Also, the pressure of the inflow stream is the same as that of the reservoir, but its temperature is determined by the upstream network.

The air compressor is modelled by the Pressure source block in Simscape. The block has two ports and is capable of maintaining a constant pressure difference between its ports. Therefore, by connecting the input port to the reservoir, a set pressure gas can be injected into the system. The given pressure remains constant regardless of the mass flow rate at the output port. The pressure source is considered isentropic, holding

$$\frac{(P_A)^{\frac{\gamma R}{c_p}}}{T_A} = \frac{(P_B)^{\frac{\gamma R}{c_p}}}{T_B} \quad (3-6)$$

By combining the abovementioned blocks, as shown in Figure 3.2, a supply unit for the considered pneumatic actuator can be modelled.

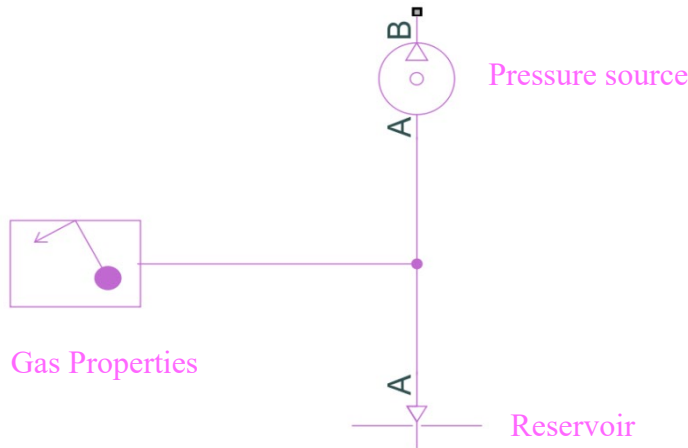


Figure 3.2. The Simscape model of the supply unit

Simscape uses the control volume approach to model gas behaviour in different parts of the system. In this approach, each pneumatic component is considered as an internal node enclosed by a control surface. The mass flow rate in the control surface can be expressed as

$$\dot{m}_{in} - \dot{m}_{out} = \frac{\partial M}{\partial P} \frac{dP_l}{dt} + \frac{\partial M}{\partial T} \frac{dT_l}{dt} \quad (3-7)$$

where \dot{m}_{in} and \dot{m}_{out} are the mass flow rate of gas entering and leaving the control surface. The gas volume properties are denoted by subscript l , such as P_l and T_l that represent the pressure and temperature of the gas volume in the internal node. This notion will be used in the rest of this chapter. $\partial M / \partial P$ is the mass flow rate of the gas volume with respect to pressure at constant temperature and volume; and $\partial M / \partial T$ is the mass flow rate of the gas volume with respect to temperature at constant pressure and volume. For an ideal gas,

$$\begin{aligned}\frac{\partial M}{\partial P} &= V \frac{\rho_l}{P_l} \\ \frac{\partial M}{\partial T} &= -V \frac{\rho_l}{T_l}\end{aligned}\quad (3-8)$$

Similarly, the control surface heat flow rate can be expressed as:

$$\Phi_{in} - \Phi_{out} + Q = \frac{\partial U}{\partial P} \frac{dP_l}{dt} + \frac{\partial U}{\partial T} \frac{dT_l}{dt} \quad (3-9)$$

where Φ_{in} and Φ_{out} are the energy flow rates due to the gas entering and leaving the control surface. Q is the heat flow rate as a result of heat transferring between the control system and its surrounding, and U is the internal energy of the gas volume in the internal node. For an ideal gas,

$$\begin{aligned}\frac{\partial U}{\partial P} &= V \left(\frac{h_l}{zRT_l} - 1 \right) \\ \frac{\partial U}{\partial T} &= V \rho_l \left(c_{pl} - \frac{h_l}{T_l} \right)\end{aligned}\quad (3-10)$$

3.3. The Pipe Model

In pneumatic pipe model, the gas pressure drop between the input and output of a pipe and the heat transfer between the gas and its surrounding environment should be demonstrated. The pressure drop at each end of the pipe is given as

$$\begin{aligned}P_{in} - P_l &= \left(\frac{\dot{m}_{in}}{A_t} \right)^2 \times \left(\frac{1}{\rho_l} - \frac{1}{\rho_{in}} \right) + \Delta P_{inl} \\ P_{out} - P_l &= \left(\frac{\dot{m}_{out}}{A_t} \right)^2 \times \left(\frac{1}{\rho_l} - \frac{1}{\rho_{out}} \right) + \Delta P_{outl}\end{aligned}\quad (3-11)$$

where A_t is the pipe's cross-sectional area, and $\Delta P_{\{\cdot\}l}$ is the pressure losses due to viscous friction, μ ($\{\cdot\}$ notation was used to abbreviate the equations and can be replaced by "in" or "out". This notation will be used in the rest of this chapter).

The pressure loss in a pipe depends on Reynolds numbers. The Reynolds number at each end of the pipe is equal to

$$Re_{\{i\}} = \frac{|\dot{m}_{\{i\}}|D}{A_t\mu_l} \quad (3-12)$$

D is the pipe's diameter. If the calculated Reynolds number is less than 2000, the gas flow follows the laminar regime, and the pressure drop is equal to [110]

$$\Delta P_{\{i\}l} = f_{shape} \frac{\dot{m}_{\{i\}} \mu_l}{2\rho_l D^2 A_t} \times \frac{L_t + L_{eqv}}{2} \quad (3-13)$$

and for Reynolds numbers greater than 4000, the gas flow follows the turbulent flow regime, with the pressure drop equal to

$$\Delta P_{\{i\}l} = f_{Darcy_{\{i\}}} \frac{\dot{m}_{\{i\}} \mu_l}{2\rho_l D A_t^2} \times \frac{L_t + L_{eqv}}{2} \quad (3-14)$$

L_t is the pipe's length and L_{eqv} is the aggregate equivalent length of local resistances, which has been taken as 10% of the pipe's length. The shape factor, f_{shape} , is considered as a constant number equal to 2.59, but the Darcy friction factor, f_{Darcy} , is a function of the Reynolds number and is equal to

$$f_{Darcy_{\{i\}}} = \left[-1.8 \log \left(\frac{6.9}{Re_{\{i\}}} + \left(\frac{\varepsilon_{rough}}{3.7D} \right)^{1.11} \right) \right]^{-2} \quad (3-15)$$

where ε_{rough} is the internal surface absolute roughness. For the Reynolds numbers between 2000 and 4000, a transition between laminar and turbulence regimes has been assumed.

The convective heat transfer between the gas flowing in the pipe and the pipe's wall can be obtained from [111] as

$$Q = \left| \frac{\dot{m}_{in} - \dot{m}_{out}}{2} \right| C_{p_{avg}} (T_H - T_{in}) \left(1 - \exp \left(- \frac{N_u \kappa_{avg} \pi L_t}{\left| \frac{\dot{m}_{in} - \dot{m}_{out}}{2} \right| C_{p_{avg}}} \right) \right) + \kappa_l \pi L_t (T_H - T_l) \quad (3-16)$$

where $C_{p_{avg}}$ and κ_{avg} are the specific heat capacity and thermal conductivity calculated at the average temperature. N_u is the Nusselt number and κ_l is the gas volume thermal conductivity. T_{in} and T_H are the inlet and pipe internal wall temperatures. The value of Nusselt number depends on the flow regime, where for the laminar flow is constant and is taken as 3.66, and for turbulence flow is equal to

$$N_{u_{tur}} = \frac{\frac{f_{Darcy}}{8} (Re_{avg} - 1000) Pr_{avg}}{1 + 12.7 \sqrt{\frac{f_{Darcy}}{8}} + Pr_{avg}^{2/3} - 1} \quad (3-17)$$

Re_{avg} and Pr_{avg} are the Reynolds and Prandtl numbers, which are obtained at the average temperature.

The conduction heat transfer in the pipe's wall can be mathematically modelled by

$$Q = \rho_t \pi D L_t C_t (T_t - T_H) \quad (3-18)$$

where ρ_t , C_t and T_t are the pipe's wall density, specific heat capacity and temperature. Finally, the convective heat transfer between the pipe's wall and the surrounding environment can be expressed as:

$$Q = \kappa_{air} \pi D L_t (T_{atm} - T_t) \quad (3-19)$$

where κ_{air} and T_{atm} are the surrounding air thermal conductivity and temperature.

The pipes can be modelled in Simscape, as is shown Figure 3.3, using the Pipe(G), Thermal Mass, Convective Heat Transfer and Temperature Source blocks. The parameters used in calculating the gas pressure drop and convective heat transfer between the gas flowing in the pipe and the pipe's wall are set in the Pipe (G) block. The pipe properties for modelling the conduction heat transfer in the pipe's wall can be adjusted in the Thermal mass block, and the parameters for modelling the convective heat transfer between the pipe's wall and the surrounding environment can be set in the Convective Heat Transfer and Temperature Source blocks. The Temperature Source can maintain the atmospheric temperature regardless of the amount of heat flow into the system.

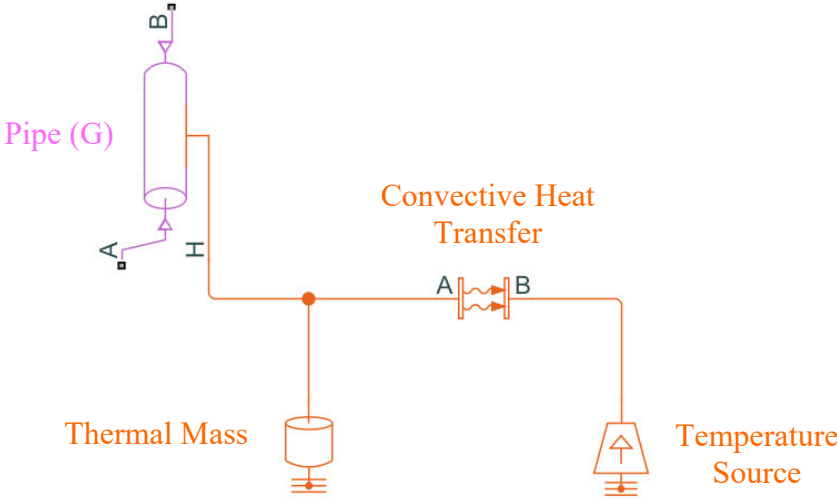


Figure 3.3. The Simscape model of the pipe

3.4. The Valve Model

The valve can be modelled as a set of restrictions capable of controlling the gas flow according to an input control signal. The restriction causes contraction of the gas at its input port, followed by the gas expansion at its output port, which results in a pressure drop across the ports. Considering the process as adiabatic, this pressure difference can be modelled as

$$\Delta P = \frac{\dot{m}_{in}}{C_d A_R} \cdot \left| \frac{\dot{m}_{in}}{\rho_R C_d A_R} \right| \left(\frac{1+r}{2} \left(1 - r \frac{\rho_R}{\rho_{in}} \right) - r \left(1 - r \frac{\rho_R}{\rho_{out}} \right) \right) \tag{3-20}$$

A_R is the cross-sectional area, and ρ_R is the gas volume density at the restriction. C_d denotes the discharge coefficient, and $r = A_R/A_{port}$ is the ratio of restriction cross-sectional area to the ports cross-sectional area. It is assumed that both ports have the same dimensions.

As is seen from equation (3-20), the pressure difference is proportional to the square of the gas flow rate, \dot{m}_{in} , which is typical in the turbulence regime. However, in the laminar regime, the pressure difference is linearly proportional to the gas flow rate, and thus ΔP can be approximated as

$$\Delta p_{lam} = \sqrt{\frac{\rho_R \cdot \frac{p_{in} + p_{out}}{2} (1 - B_{lam})}{2}} (1 - r) \quad (3-21)$$

where p_{in} and p_{out} are the pressure of the inflow and outflow gases into the restriction, and B_{lam} is the laminar flow pressure ratio, which is taken as constant 0.999.

The amount of pressure at the restriction is equal to

$$P_R = p_{in} - \frac{\dot{m}_{in}}{C_d A_R} \cdot \left| \frac{\dot{m}_{in}}{\rho_R C_d A_R} \right| \left(\frac{1+r}{2} \left(1 - r \frac{\rho_R}{\rho_{in}} \right) \right) \quad (3-22)$$

and for the laminar regime this can be approximated as

$$P_R = \frac{p_{in} + p_{out}}{2} - \frac{1}{\rho_R} \left(\frac{\dot{m}_{in}}{C_d A_R} \right)^2 \frac{1 - r^2}{2} \quad (3-23)$$

The Local Restriction (G) block has been used for modelling the valve in the Simscape environment. Each active state of the valve can be modelled by two local restriction blocks connecting ports P and T to ports A and B. The block allows modelling the valve leakage by defining a non-zero minimum restriction area, $A_{leakage}$. Moreover, the valve spool displacement, x , has been used to adjust the orifice area. The orifice cross-sectional area is linearly proportional to the spool displacement as

$$A_R = \frac{A_{max} - A_{leakage}}{x_{max} - x_{leakage}} (x - x_{leakage}) + A_{leakage} \quad (3-24)$$

where x_{max} is the maximum spool displacement causing the maximum cross-sectional area, A_{max} , in the restriction, and $x_{leakage}$ is the minimum value for the spool displacement. Figure 3.4 shows the model of the valve using Simscape components.

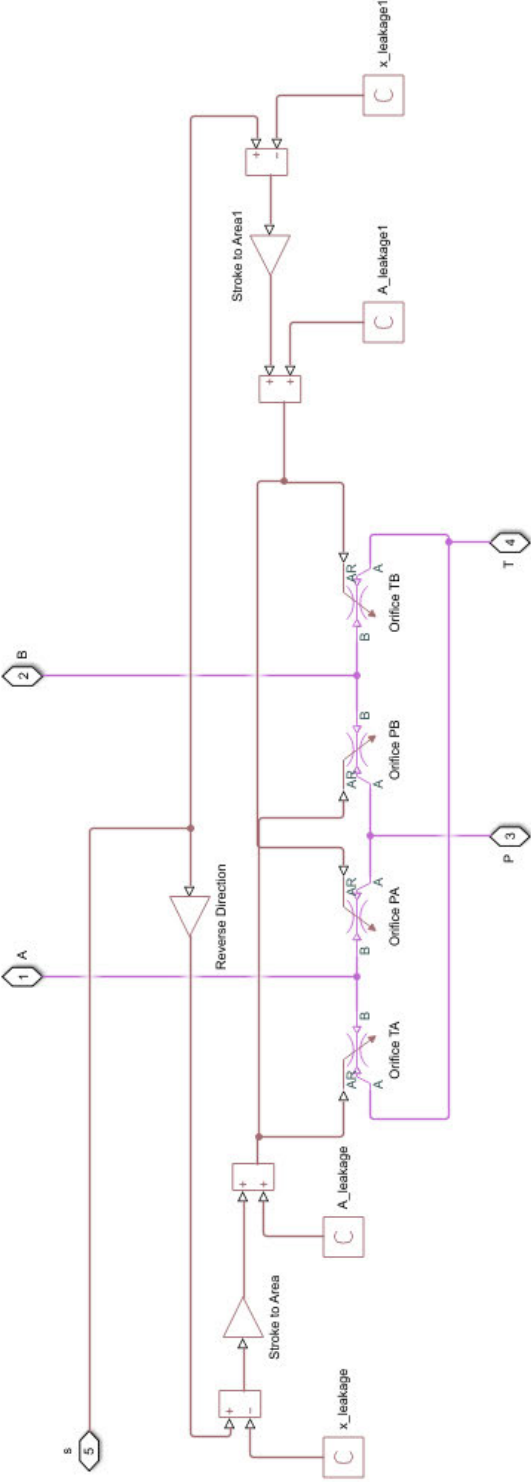


Figure 3.4. The Simscape model of the valve

3.5. The Cylinder Model

Each cylinder chamber can be considered as an internal node, with a mass flow rate of

$$\dot{m} = \frac{\partial M}{\partial p} \cdot \frac{dp_l}{dt} + \frac{\partial M}{\partial T} \cdot \frac{dT_l}{dt} + \rho_l \frac{dV}{dt} \quad (3-25)$$

and heat flow rate of

$$\phi + Q = \frac{\partial U}{\partial p} \cdot \frac{dp_l}{dt} + \frac{\partial U}{\partial T} \cdot \frac{dT_l}{dt} + \rho_l h_l \frac{dV}{dt} \quad (3-26)$$

where ϕ is the energy flow rate as a result of the gas transportation into/out of the chamber, and Q is due to the convective heat transfer between the gas in the chamber and the cylinder's body. The partial derivative terms in equations (3-25) and (3-26) can be obtained from equations (3-8) and (3-10), respectively. Equations (3-16)-(3-19) are also applicable here to model the heat transfer between the gas in the chamber and the surrounding environment.

The gas volume in the chamber depends on the displacement of the moving interface, and is equal to

$$V = V_d \pm A_p y \quad (3-27)$$

V_d denotes the dead volume, and A_p and y represent the interface cross-sectional area and displacement. The sign of the displacement value depends on the movement direction of the interface. The applied force to the interface can be expressed as:

$$F = (p_{atm} - p_l)A_p \quad (3-28)$$

where p_{atm} is the atmospheric pressure. Therefore, the total force caused by the gas pressure in chambers 1 and 2, considering the forces' directions, is equal to

$$F_p = (p_{l1} - p_{l2})A_p \quad (3-29)$$

The motion equation for the load connected to the piston rod is equal to

$$(M_L + M_P)\dot{x}_c = F_p - \beta \frac{dx_c}{dt} \quad (3-30)$$

where x_c denotes the rod's displacement, and M_L and M_P are the load and piston masses, respectively. β represents the viscous friction coefficient for the piston movement.

The Translational Mechanical Converter (G) block can be used to model each chamber. This block can model the relation between the gas pressure inside a chamber and the applied mechanical force to the interface. Moreover, a Translational Hard Stop block is used to restrict the cylinder interface movement within the length of the cylinder. The viscous friction coefficient for the piston movement can be modelled by a Translational Damper block, and Mass blocks are used for modelling the load and piston masses. The Convective heat transfer, Thermal mass and Temperature source blocks are also used to model the heat transfer between the chamber gases and the surrounding environment. The complete model for the cylinder using Simscape blocks is depicted in Figure 3.5.

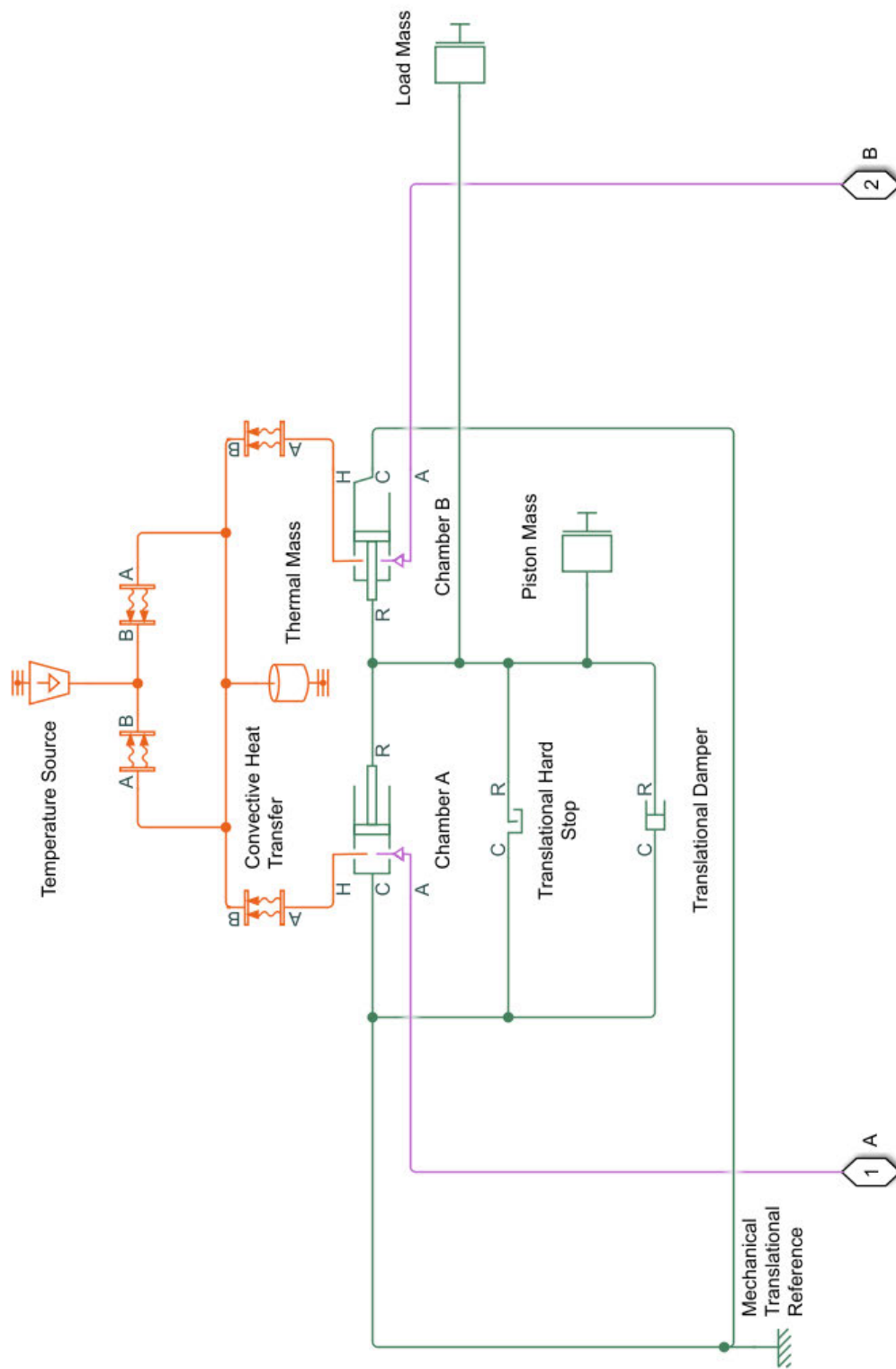


Figure 3.5. The Simscape model of the cylinder

3.6. The Simulation of the Pneumatic System

The parameters' values used for simulating the piston-cylinder pneumatic actuator that was modelled in previous sections are given in Table 3.1.

Table 3.1. Parameters values used in simulation

	Parameter Name	Parameter Value
Gas Properties	Supply pressure (P_s)	7×10^5 (Pa)
	Supply temperature (T_s)	293.15 (K)
	Gas constant (R)	287 (J/(kg.K))
	Specific enthalpy (h)	293.6 (kJ/kg)
	Compressibility factor (z)	0.999
	Specific heat capacity (C_p)	1.01 (kJ/(kg.K))
	Thermal conductivity (κ)	25.7 (mW/(K.m))
	Dynamic viscosity (μ)	18.2 (μ Pa.s)
	Specific heat ratio (γ)	1.4
	Reference temperature (T_0)	293.15 (K)
	Atmosphere pressure (P_{atm})	1×10^5 (Pa)
Valve Properties	Discharge coefficient (C_d)	0.82
	Max orifice area (A_{max})	4×10^{-6} (m ²)
	Leakage area ($A_{leakage}$)	1×10^{-10} (m ²)
	Displacement for leakage area ($X_{leakage}$)	2×10^{-4} (m)

	Displacement limit (x_{\max})	5×10^{-3} (m)
	Input voltage range	[-12,12] (V)
Pipe Properties	Length (L_t)	1 (m)
	Pipe cross-sectional area (A_t)	5×10^{-6} (m)
	Internal surface absolute roughness (ϵ_{rough})	15×10^{-6} (m)
	Pipe wall density (ρ_t)	1500 (kg/m ³)
	Pipe wall specific heat capacity (C_t)	1250 (J/(kg.K))
	Wall-air heat transfer coefficient (κ_{air})	20 (W/(m ² .K))
Cylinder Properties	Initial interface displacement (L_{init})	0 (m)
	Max piston stroke (L_p)	0.2 (m)
	Interface cross-sectional area (A_p)	0.002 (m ²)
	Dead volume (V_d)	4×10^{-5} (m ³)
	Gas-wall heat transfer coefficient (κ_p)	100 (W/(m ² .K))
	Actuator wall specific heat ($C_{Cylinder}$)	870 (J/(kg.K))
	Actuator mass (M_C)	3 (kg)
	Piston mass (M_P)	1 (kg)

	Hard stop stiffness (k_{hs})	1×10^7 (N/m)
	Hard stop damping (β_{hs})	1500 (N/(m.s))
	Mechanical damping (β_{Mech})	200 (N/(m.s))

As is given in equation (3-1), the gas density varies according to its pressure and temperature. The changes in the dry air density with respect to changes in its pressure and temperature is simulated and shown in Figure 3.6. The ranges of temperature and pressure are selected according to their potential values during the operation of the system.

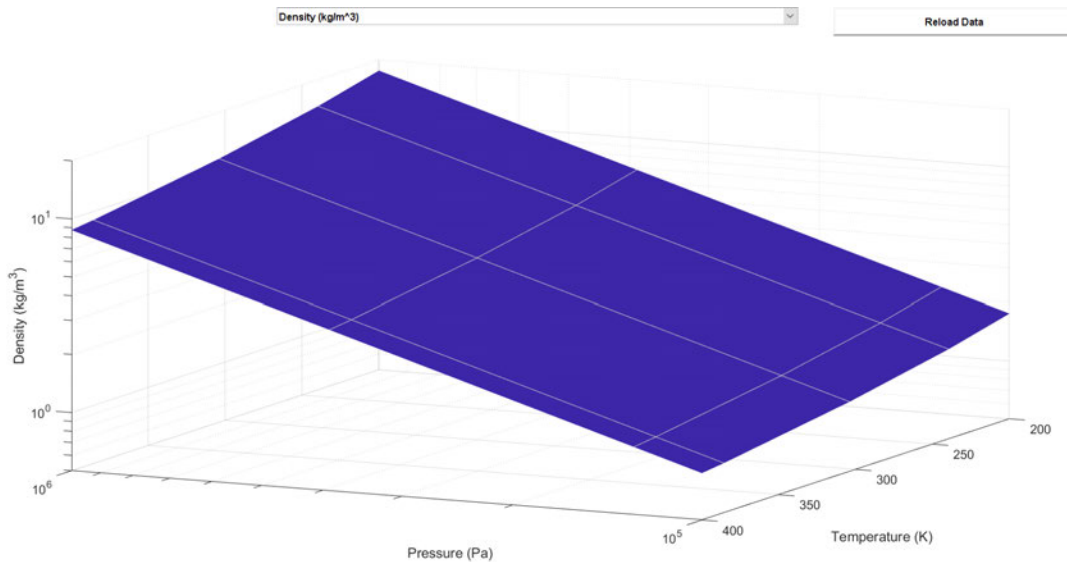


Figure 3.6.The gas property plot for dry air considered in the simulation

We then apply an input voltage to the valve and measure the rod's displacement. This is depicted in Figure 3.7. The input signal is selected in such a way as to take the valve's spool to its extreme positions. An applied 12V signal charges chamber 1 and allows gas to be exhausted from chamber 2, which causes the rod to extend to its maximum displacement, 0.2m. The signal has been applied long enough so that the system can be settled. The valve is then moved to its neutral state by applying 0V, and as is shown, the rod's displacement remains unchanged. By applying -12V to the valve, the gas in chamber 1 exhausts, and chamber 2 fills with gas, moving the piston inward until it reaches zero. Again, a 0V signal has been applied to move the valve

to its neutral state, where holding the rod's position unchanged. The response transition time is 2s.

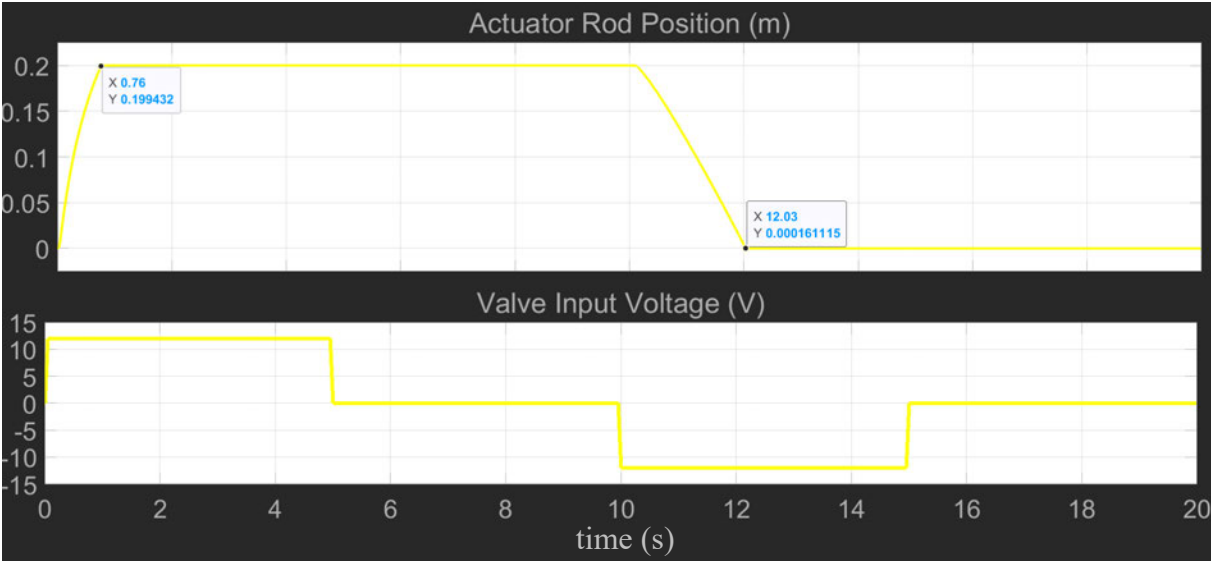


Figure 3.7. Effect of the valve's input voltage on the rod's displacement

The pneumatic pipes model demonstrates the gas pressure drop between the input and output of a pipe and the heat transfer between the gas and its surrounding environment. Figure 3.8, Figure 3.9, Figure 3.10 and Figure 3.11 depict the pressure and temperature difference between pipes' gas volume and the inflow and outflow gases in the supply pipe, exhaust pipe, pipe A and pipe B, respectively.

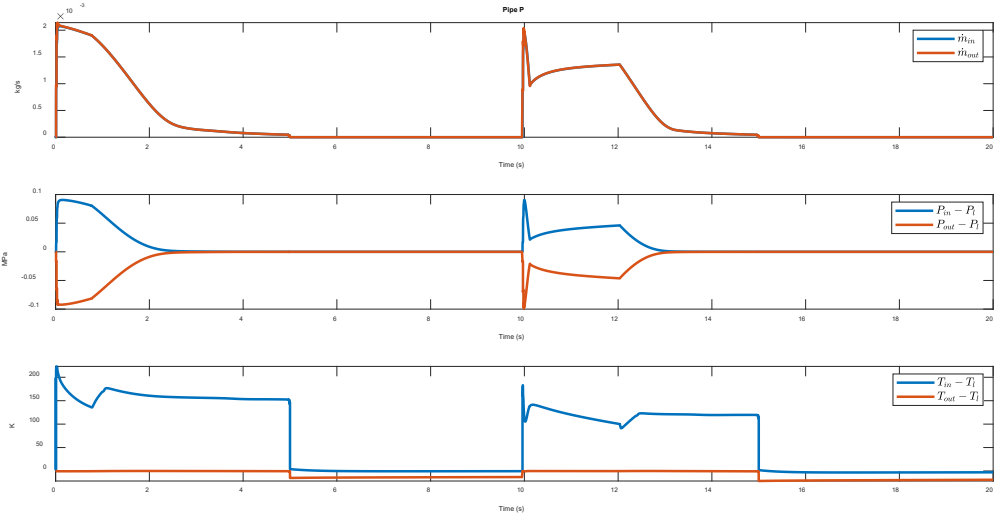


Figure 3.8. Pressure drop and temperature difference across the supply pipe (P)

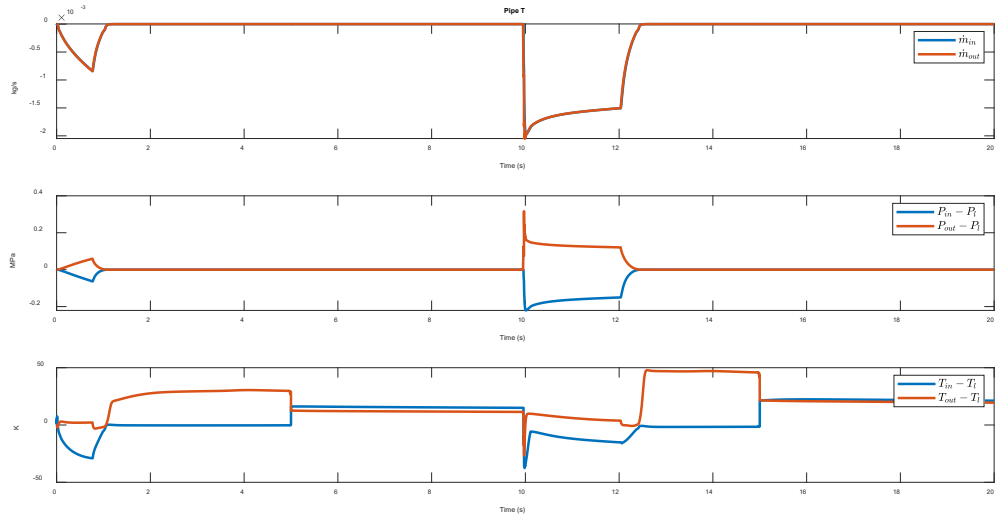


Figure 3.9. Pressure drop and temperature difference across the exhaust pipe (T)

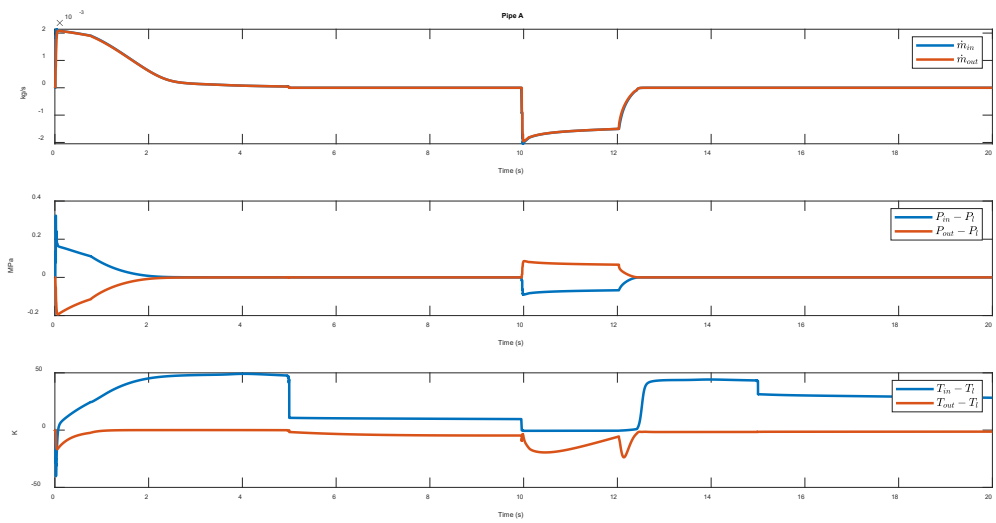


Figure 3.10. Pressure drop and temperature difference across pipe (A)

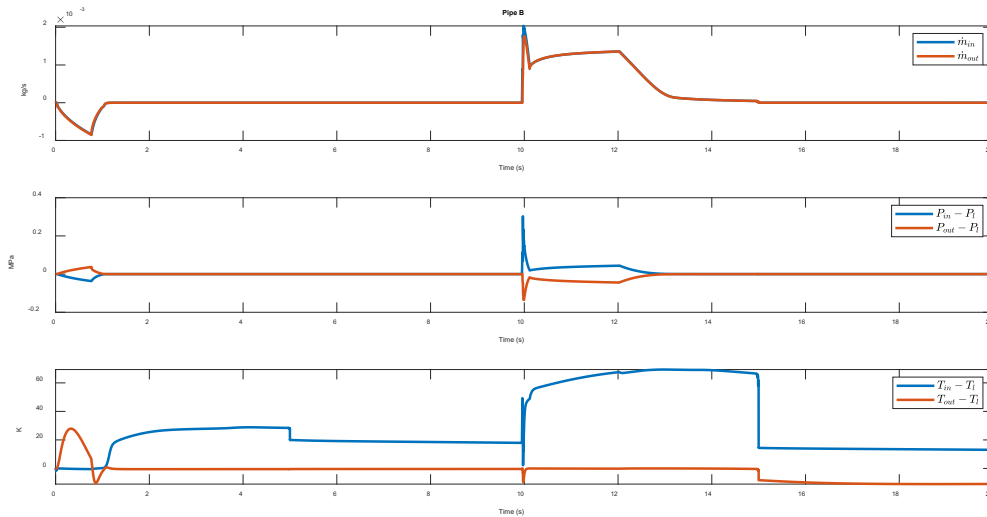


Figure 3.11. Pressure drop and temperature difference across pipe (B)

Next, the effect of applied voltage on the valve’s cross-sectional area has been simulated and shown in Figure 3.12. For the negative values of the applied voltage, the valve supplies port B, and for the positive values, it connects the supply port P to port A. As is seen, a dead-band behaviour appears in the vicinity of 0V.

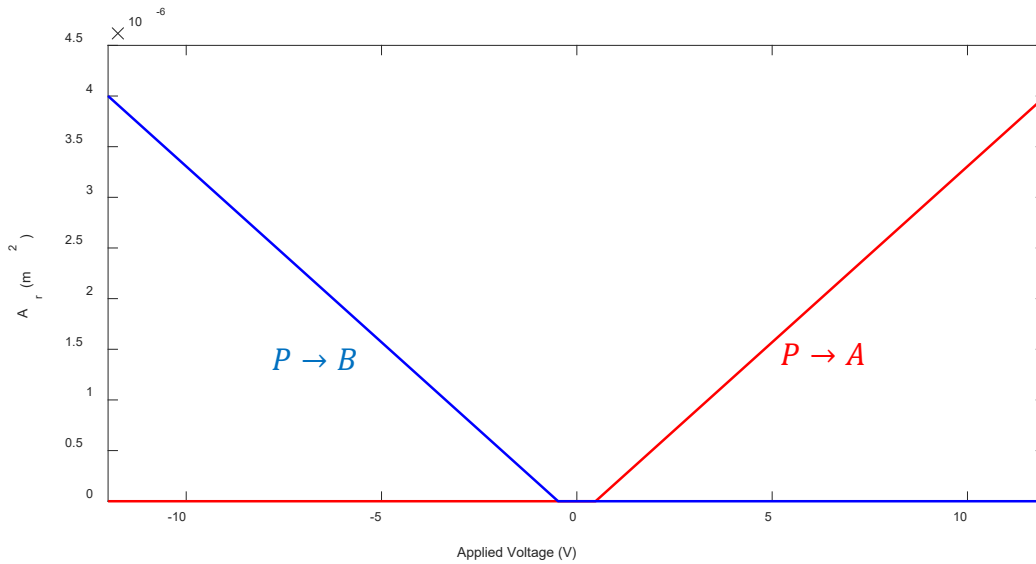


Figure 3.12. Changes in the input valve cross-sectional area with the applied voltage.

The gas flow rate, \dot{m}_{in} , in the valve with respect to the applied voltage values is given in Figure 3.13. As a result of leakage, the gas flow rate for the applied voltage less than 0.5V remains at zero. By applying more voltage, the gas flow rate increases by following a laminar

regime until it reaches a point that the flow rate enters into a turbulence regime, in which a decrease in the flow rate slope can be observed.

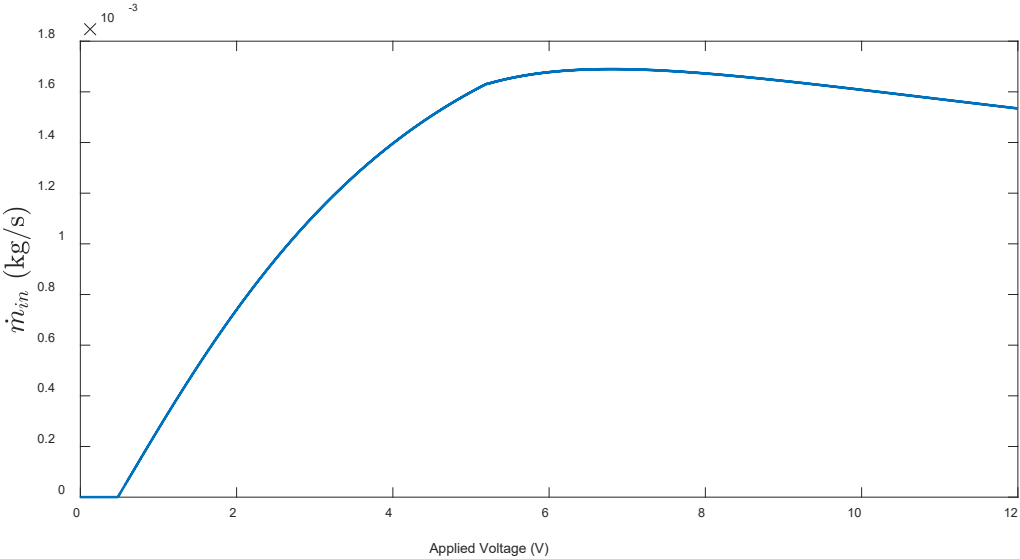


Figure 3.13. Mass flow rate in the valve versus the applied voltage

The changes in the cylinder’s chamber 1 and chamber 2 gas pressure, temperature and volume as a result of applied voltage given in Figure 3.7 are shown in Figure 3.14 and Figure 3.15, respectively. The effect of considering a dead volume for the cylinders can be observed from their volume graphs.

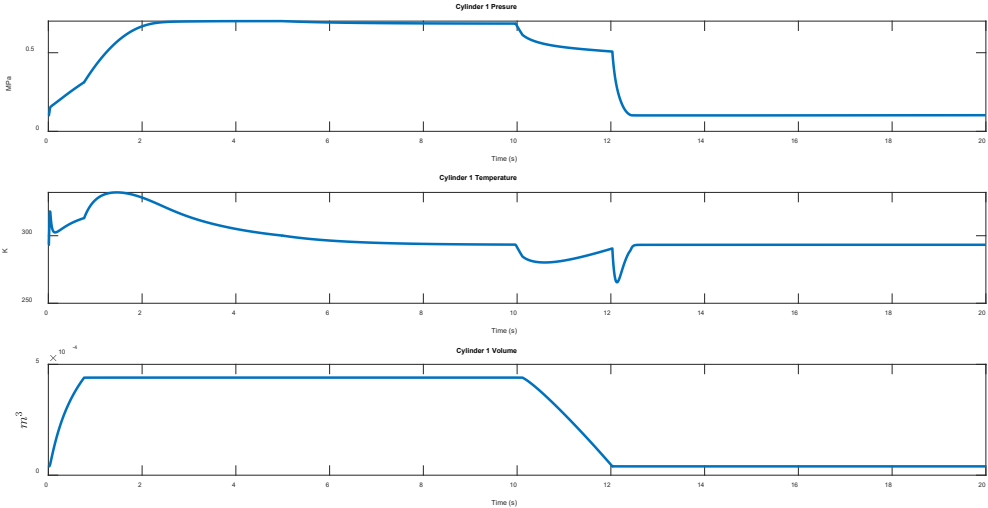


Figure 3.14. Changes of pressure, temperature and volume in Chamber 1

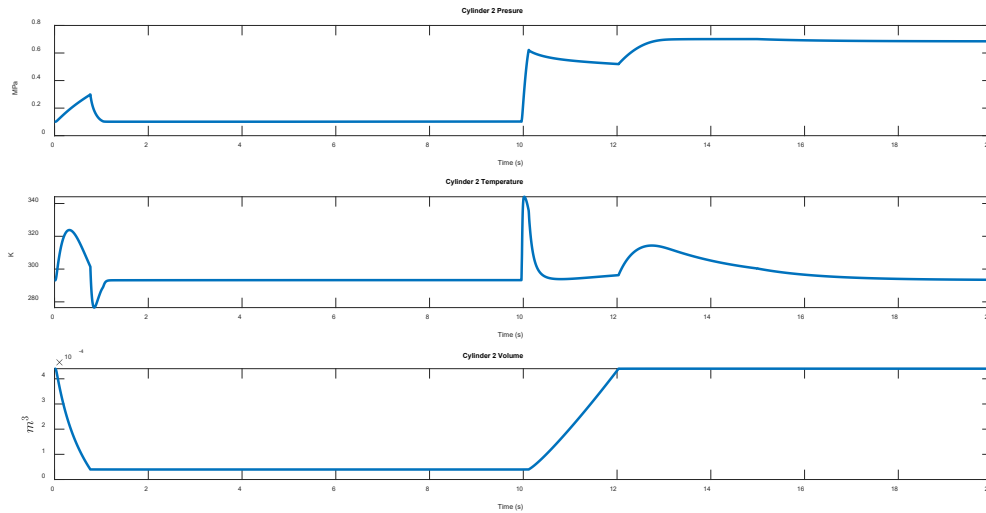


Figure 3.15. Changes of pressure, temperature and volume in Chamber 2

Finally, the frequency response of the system has been studied. As was discussed, the air is compressible and has a low damping characteristic, which causes a nonlinear response and increases the pneumatic system's dynamic order. Moreover, before the system can apply any force to a load, the pipes and cylinders have to be filled with air. This results in further nonlinearities in the form of dead-band and transmission attenuations. Also, a pneumatic system is affected by frictional forces caused by the mechanical parts' movements. All these uncertainties and nonlinearities make linearizing a pneumatic system a complicated practice that generates inaccurate results. Therefore, a system identification approach has been implemented to estimate the frequency response of the pneumatic actuator. In this approach, a set of sinusoidal signals with different frequencies would be applied to the system and the piston's rod displacement would be measured. The collected results are then used to draw the system's bode plot. The estimated bode plot for the pneumatic actuator obtained by applying sinusoidal voltage signals in the range of 0.5 to 100Hz is given in Figure 3.16, showing around 1.6rad/s frequency bandwidth for the considered pneumatic actuator.

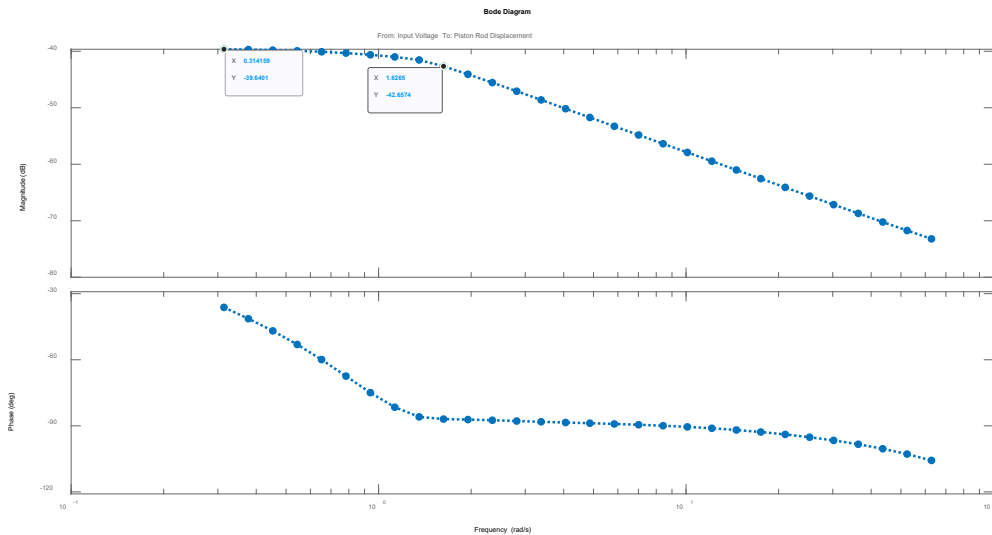


Figure 3.16. The pneumatic system estimated frequency response

3.7. Summary

In this chapter, the mathematical model of a double-acting pneumatic cylinder controlled by a 4/3 electro-pneumatic valve were obtained. The nonlinearities and uncertainties, which are part of the physical properties of such a system were discussed and included in the model. For this purpose, different theoretical analysis, including thermodynamics, fluid mechanics and motion dynamics theories have been used. Moreover, the details for simulating the system in MATLAB SimScape were discussed. According to a set of selected parameters, the simulation results were then presented, demonstrating the effect of system nonlinearities on the system's response.

CHAPTER 4: ITERATIVE LEARNING CONTROLLER DESIGN

4.1. Introduction

This chapter covers the procedure for designing a controller for the considered pneumatic actuator covered in Chapter 3. First, the performance of the system controlled by a conventional PID controller will be studied. This follows by providing an overview of the ILC theory. Then the design of the ILC method for controlling the actuator is discussed, and its performance is studied based on theoretical analysis and simulation results. Finally, a comparison between the performance of the designed controllers is provided. According to [112], servo pneumatic actuators in approximately 70% of industrial applications should move 1-10 kg payloads with ± 2 to ± 0.02 mm precision. Therefore, in this chapter, we consider the same criteria in studying the performance of the designed controllers.

4.2. PID Controller Design for the Pneumatic Actuator

An accurate or well-estimated model of the plant is required to design a well-tuned PID controller. Therefore, we use the obtained frequency response of the system, which is shown in Figure 3.16, to design a PID controller for the pneumatic actuator. We further use frequency domain techniques, namely Nichols chart and Inverse Nichols chart, to achieve the required performance in reference tracking and disturbance rejection.

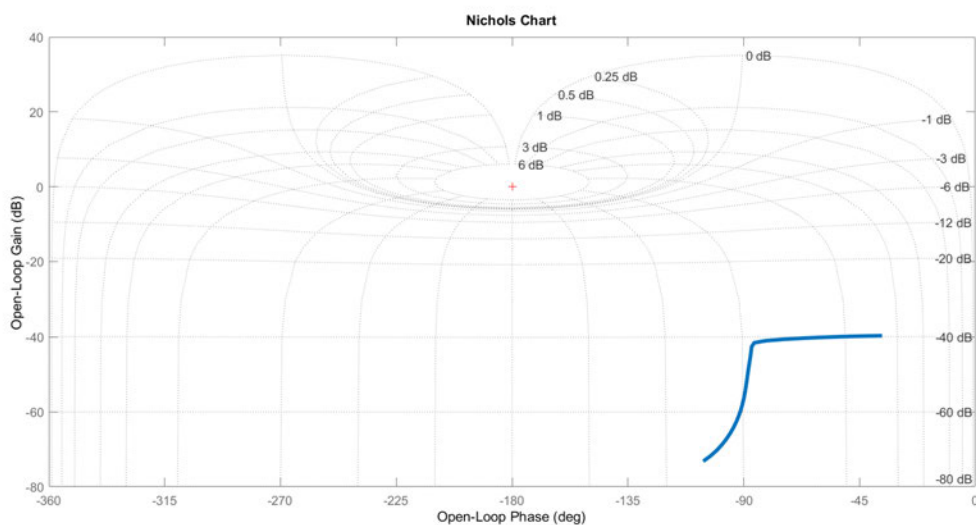


Figure 4.1. Nichols Chart of the plant

The Nichols Chart of the actuator using the frequency response of the estimated system is shown in Figure 4.1. We use a parallel form of the PID controller as

$$C(s) = P + \frac{I}{s} + D \frac{N}{1 + N \frac{1}{s}} \quad (4-1)$$

P , I and D are the proportional, integrator and differentiator gains, and N is the filter coefficient to realize the derivative term. To obtain the precision of $\pm 0.002\text{m}$ for the considered actuator, the tracking boundaries should be in the range of

$$20 \log\left(\frac{0.2 - 0.002}{0.2}\right) \leq TB_{dB} \leq 20 \log\left(\frac{0.2 + 0.002}{0.2}\right) \quad (4-2)$$

$$-0.09\text{dB} \leq TB_{dB} \leq 0.08\text{dB}$$

As is seen in Figure 4.2, the controller given in (4-3) can achieve the tracking boundaries for the lower frequencies ($\omega < 0.6 \text{ rad/s}$). The performance of the system in tracking a reference signal is shown in Figure 4.3.

$$C(s) = 100 + \frac{10}{s} + \frac{8}{1 + 8 \frac{1}{s}} \quad (4-3)$$

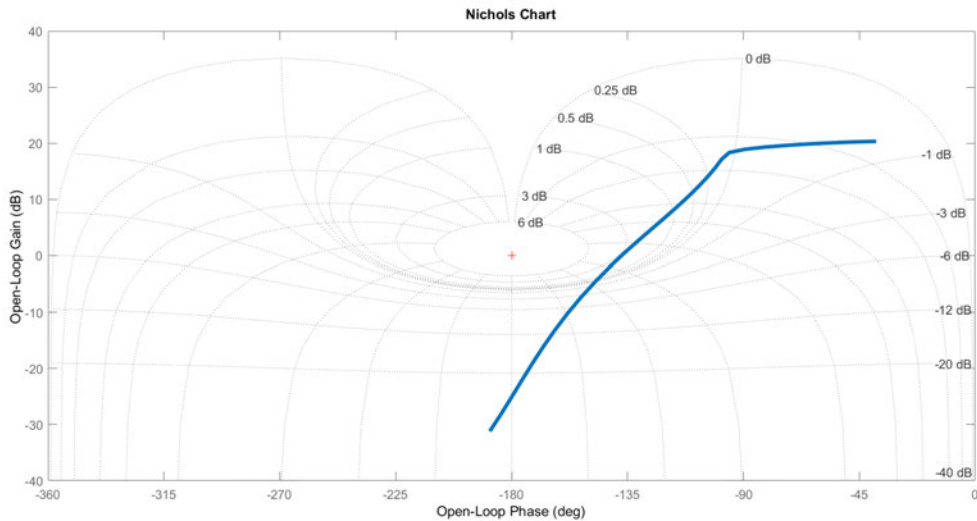


Figure 4.2. Nichols chart of the PID controlled actuator

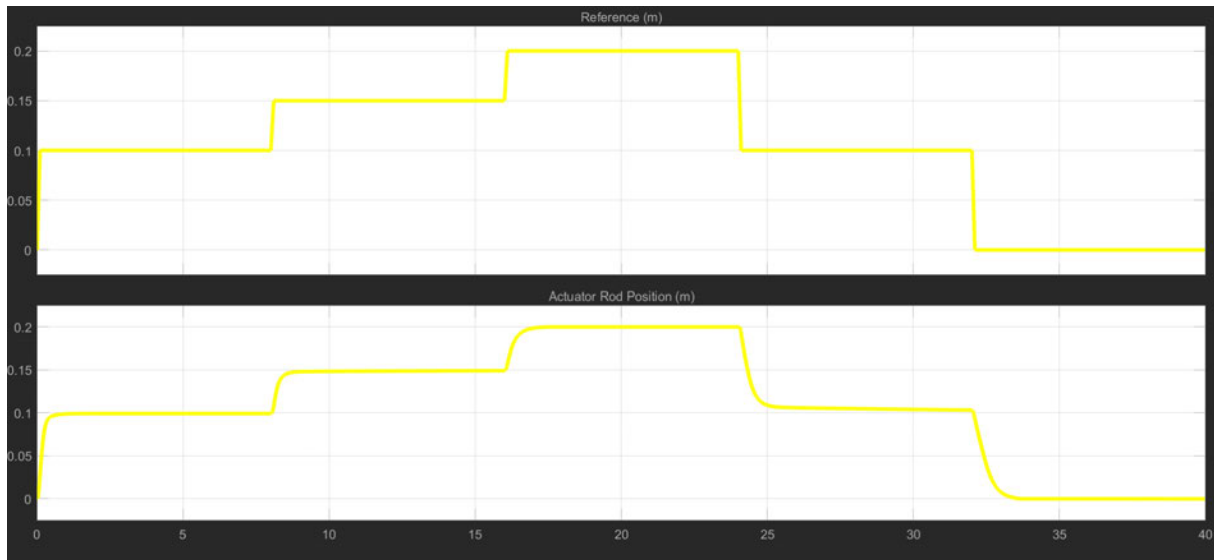


Figure 4.3. Tracking performance of the PID controlled actuator

The difference between the reference and output of the system is shown in Figure 4.4 showing the tracking requirement has been achieved at the steady state. Nevertheless, the system shows around a 0.75s delay to obtain the $\pm 0.002\text{m}$ precision.

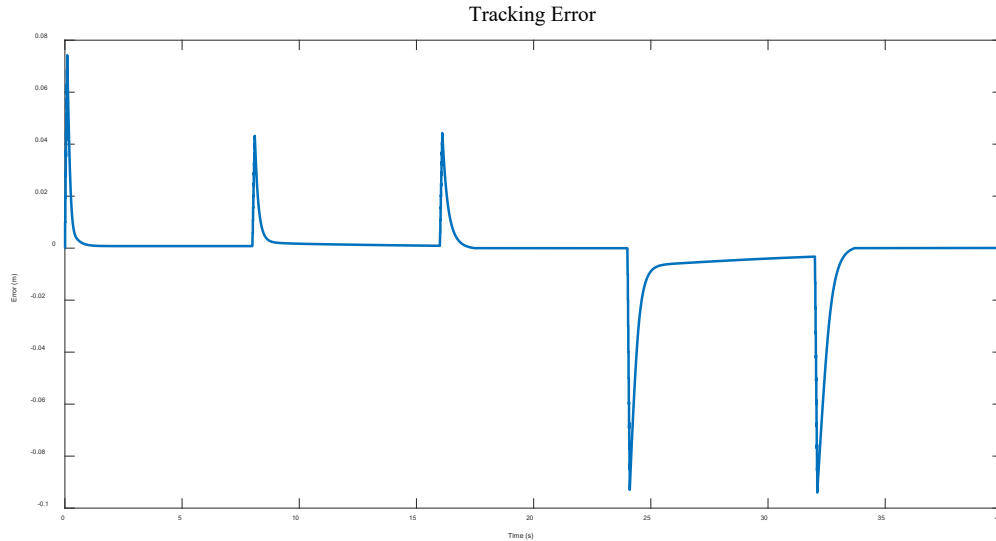


Figure 4.4. Tracking error for the PID controlled actuator

Next, we investigate the performance of the system to overcome uncertainties. For this purpose, we first study the controller performance based on the Inverse Nichols chart, as is shown in Figure 4.5. As is seen, the sensitivity bound for the lower frequencies ($\omega < 8 \text{ rad/s}$)

is less than 3dB and for all frequencies is less than 6dB. The performance of the system in overcoming the payload uncertainty is demonstrated in Figure 4.6, showing that the controller cannot maintain the required precession ($\pm 0.002\text{m}$) as a result of changes in the load.

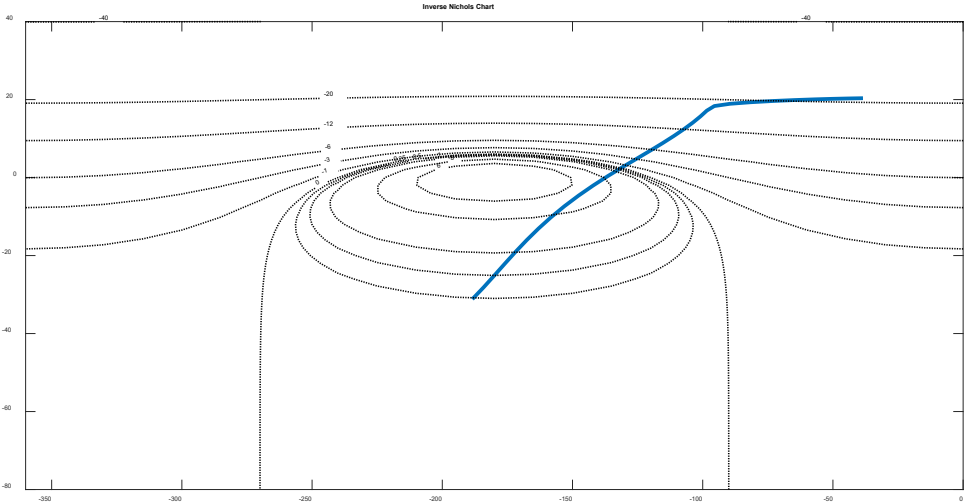


Figure 4.5. Inverse Nichols chart of the PID controlled actuator

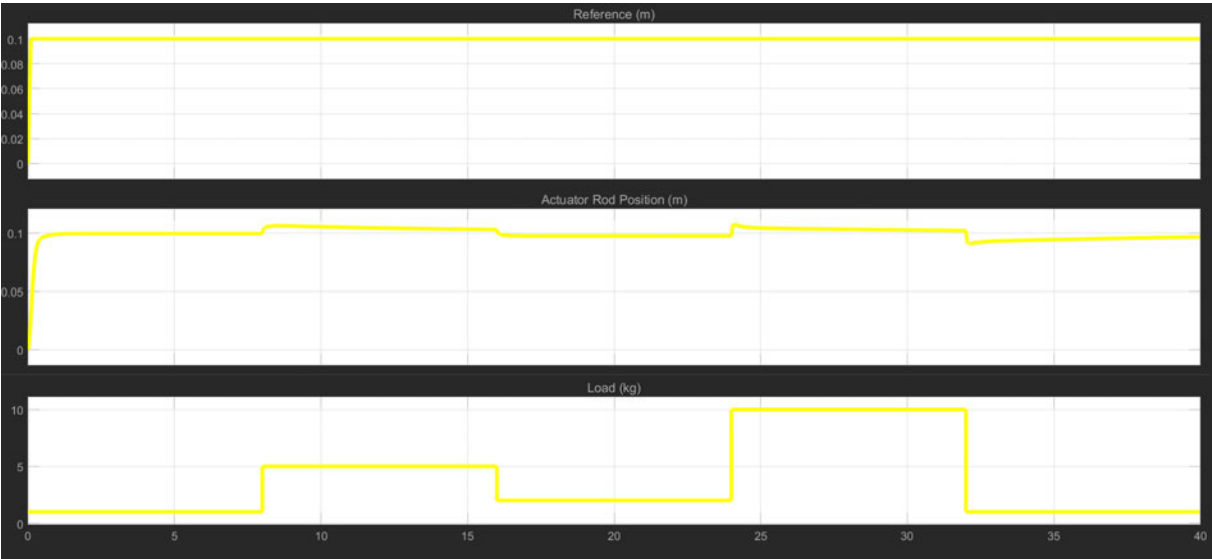


Figure 4.6. Performance of the PID controlled actuator under payload uncertainty

4.3. Iterative Learning Control Techniques

The ILC method can be applied to repetitive processes. In such processes, every iteration starts and ends at the same conditions and lasts for a fixed period of time, T . The state-space

equation for a repetitive linear time-invariant system (with no feedthrough) can be represented as

$$\begin{aligned} \dot{\mathbf{x}}_k(t) &= \mathbf{A}_c \mathbf{x}_k(t) + \mathbf{B}_c u_k(t) ; t \in [0, T] \quad \mathbf{x}_k(0) = \mathbf{x}_0 \quad \forall k \\ y_k(t) &= \mathbf{C}_c \mathbf{x}_k(t) \end{aligned} \quad (4-4)$$

$k > 0$ denotes the trial number, and $\mathbf{x}_k(t) \in \mathbb{R}^n$, $y_k(t) \in \mathbb{R}$ and $u_k(t) \in \mathbb{R}$ respectively represent the state variable vector, output and input of the system at the k^{th} iteration. Suppose the system's desired output for every iteration is $y_d(t)$, which makes the error at the k^{th} iteration equal to

$$e_k(t) = y_d(t) - y_k(t) \quad (4-5)$$

The idea of the ILC is to define a control law using previous trials' information such that the error monotonically decreases in every new iteration until it reaches zero ($\lim_{k \rightarrow \infty} e_k(t) = 0$). A general architecture for an ILC-controlled system is shown in Figure 4.7. The control signal is calculated according to a recursive law as

$$u_{k+1}(t) = F(u_0(t'), \dots, u_k(t'), y_0(t'), \dots, y_k(t'), y_d(t')) ; 0 \leq t' \leq T \quad (4-6)$$

If F is designed in a way that $t' > t$, then the learning law is known as noncausal. Moreover, the control signal generated at the $(k + 1)^{th}$ iteration can be calculated based on the information collected from all previous iterations. This method is called the high-order ILC (HOILC). However, a simplified law is preferred as long as it can attain the convergence with satisfactory speed.

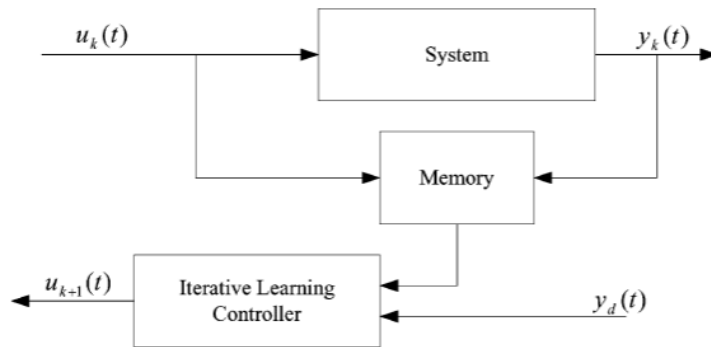


Figure 4.7. ILC Architecture

The ILC algorithm can be presented in discrete-time, which is more suitable for being implemented by a microcontroller. For a sampling time of T_s , where $T = NT_s$, the system can be considered as

$$\begin{aligned} \mathbf{x}_k[i+1] &= \mathbf{A}\mathbf{x}_k[i] + \mathbf{B}u_k[i]; \quad i \in [0, N] \quad \mathbf{x}_k[0] = \mathbf{x}_0 \quad \forall k \\ y_k[i] &= \mathbf{C}\mathbf{x}_k[i] \end{aligned} \quad (4-7)$$

$$\mathbf{A} = e^{\mathbf{A}_c T_s}, \quad \mathbf{B} = \int_0^{T_s} e^{\mathbf{A}_c \alpha} d\alpha \mathbf{B}_c \quad \text{and} \quad \mathbf{C} = \mathbf{C}_c.$$

The system's output can be calculated as

$$y_k[i] = \mathbf{C}(q\mathbf{I} - \mathbf{A})^{-1} \mathbf{B} u_k[i] + \mathbf{C}\mathbf{A}^k \mathbf{x}_0 = P(q)u_k[i] + d_k \quad (4-8)$$

where q denotes the forward time-shift operator as $qx[i] \equiv x[i+1]$.

For a rational LTI system, $P(q)$ can be expanded into

$$P(q) = \mathbf{C}\mathbf{B}q^{-1} + \mathbf{C}\mathbf{A}\mathbf{B}q^{-2} + \mathbf{C}\mathbf{A}^2\mathbf{B}q^{-3} + \dots \quad (4-9)$$

and the error at the k^{th} iteration is equal to

$$e_k[i] = y_d[i] - y_k[i] \quad (4-10)$$

The ILC control law in the discrete-time domain can then be presented as

$$u_{k+1}[i] = F(u_k[\cdot], \dots, u_0[\cdot], y_k[\cdot], \dots, y_0[\cdot], y_d[\cdot]) \quad (4-11)$$

where $[\cdot]$ represents any sample in the range of $[0, N]$. In such cases, it is common to implement the ILC method in the form of digital filters. Figure 4.8 shows an example of an ILC structure with the ILC law of

$$u_{k+1}[i] = Q(q)(L(q)(y_d[i] - y_k[i]) + u_k[i]) + C(q)(y_d[i] - y_{k+1}[i]) \quad (4-12)$$

The control signal is generated using the current, $k+1$, and the past iteration, k , information. The learning functions can be causal or noncausal as

$$\begin{aligned}
Q(q) &= \dots + q_{-2}q^{-2} + q_{-1}q^{-1} + q_0 + q_1q^{-1} + q_2q^{-2} + \dots \\
L(q) &= \dots + l_{-2}q^{-2} + l_{-1}q^{-1} + l_0 + l_1q^{-1} + l_2q^{-2} + \dots \\
M(q) &= \dots + m_{-2}q^{-2} + m_{-1}q^{-1} + m_0 + m_1q^{-1} + m_2q^{-2} + \dots
\end{aligned} \tag{4-13}$$

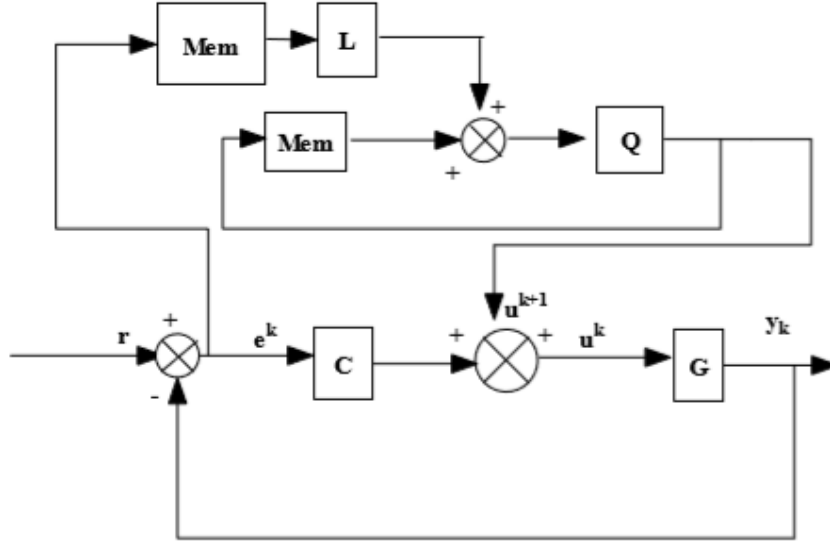


Figure 4.8. Example of an ILC structure

4.4. Controller Design

We begin our design by considering a general form for the ILC law as

$$u_{k+1}[i] = Q(q)u_k[i] + L(q)y_k[i] + M(q)y_d[i] \tag{4-14}$$

To represent (4-14) in matrix format, let us consider N sample sequences for the input, output and desired signals as

$$\begin{aligned}
\mathbf{u}_k &= [u_k[0] \quad u_k[1] \quad \dots \quad u_k[N-1]]^T \\
\mathbf{y}_k &= [y_k[1] \quad y_k[2] \quad \dots \quad y_k[N]]^T \\
\mathbf{y}_d &= [y_d[1] \quad y_d[2] \quad \dots \quad y_d[N]]^T \\
\mathbf{d}_k &= [d_k \quad d_k \quad \dots \quad d_k]^T
\end{aligned} \tag{4-15}$$

and \mathbf{M} , \mathbf{L} , \mathbf{Q} and \mathbf{P} as matrices equal to

$$\begin{aligned}
\mathbf{M} &= \begin{bmatrix} m_0 & m_{-1} & \dots & m_{-(N-1)} \\ m_1 & m_0 & \dots & m_{-(N-2)} \\ \vdots & \vdots & \ddots & \vdots \\ m_{N-1} & m_{N-2} & \dots & m_0 \end{bmatrix} & \mathbf{L} &= \begin{bmatrix} l_0 & l_{-1} & \dots & l_{-(N-1)} \\ l_1 & l_0 & \dots & l_{-(N-2)} \\ \vdots & \vdots & \ddots & \vdots \\ l_{N-1} & l_{N-2} & \dots & l_0 \end{bmatrix} \\
\mathbf{Q} &= \begin{bmatrix} q_0 & q_{-1} & \dots & q_{-(N-1)} \\ q_1 & q_0 & \dots & q_{-(N-2)} \\ \vdots & \vdots & \ddots & \vdots \\ q_{N-1} & q_{N-2} & \dots & q_0 \end{bmatrix} & \mathbf{P} &= \begin{bmatrix} P_1 & 0 & \dots & 0 \\ P_2 & P_1 & \dots & 0 \\ \vdots & \vdots & \ddots & \vdots \\ P_N & P_{N-1} & \dots & P_1 \end{bmatrix}
\end{aligned} \tag{4-16}$$

Therefore, (4-14) can be represented as

$$\begin{aligned}
\mathbf{u}_{k+1} &= \mathbf{Q}\mathbf{u}_k + \mathbf{L}\mathbf{y}_k + \mathbf{M}\mathbf{y}_d \\
&= (\mathbf{Q} + \mathbf{L}\mathbf{P})\mathbf{u}_k + (\mathbf{M}\mathbf{y}_d + \mathbf{L}\mathbf{d}_k)
\end{aligned} \tag{4-17}$$

An ILC method is regarded to be asymptotically stable (AS) if

$$\exists \bar{u} \in \mathbb{R} : |\mathbf{u}_{k+1}[i]| \leq \bar{u} \quad \forall k > 0, \forall i \in [1, N-1] \tag{4-18}$$

The converged control signal can be defined as $\mathbf{u}_\infty[i] = \lim_{k \rightarrow \infty} \mathbf{u}_k[i]$, and in order for (4-17) to be AS,

$$\rho(\mathbf{Q} + \mathbf{L}\mathbf{P}) < 1 \tag{4-19}$$

where $\rho(\mathbf{A}) = \max_j |\lambda_j(\mathbf{A})|$ and $\lambda_j(\mathbf{A})$ is the j^{th} eigenvalue of matrix \mathbf{A} .

The asymptotic error of the controlled system using (4-10) is equal to

$$\begin{aligned}
\mathbf{e}_\infty &= \mathbf{y}_d - \mathbf{P}\mathbf{u}_\infty - \mathbf{d}_\infty \\
&= (\mathbf{I} - \mathbf{P}(\mathbf{I} - \mathbf{Q} - \mathbf{L}\mathbf{P})^{-1}\mathbf{M})\mathbf{y}_d - (\mathbf{P}(\mathbf{I} - \mathbf{Q} - \mathbf{L}\mathbf{P})^{-1}\mathbf{L} + \mathbf{I})\mathbf{d}_\infty
\end{aligned} \tag{4-20}$$

where \mathbf{I} is an $N \times N$ identity matrix, and \mathbf{u}_∞ is calculated from (4-17) as

$$\mathbf{u}_\infty = (\mathbf{I} - \mathbf{Q} - \mathbf{L}\mathbf{P})^{-1}(\mathbf{M}\mathbf{y}_d + \mathbf{L}\mathbf{d}_\infty) \tag{4-21}$$

Proof:

$$\begin{aligned} \mathbf{u}_\infty &= (\mathbf{Q} + \mathbf{LP})\mathbf{u}_\infty + (\mathbf{M}\mathbf{y}_d + \mathbf{L}\mathbf{d}_k) \\ \therefore \mathbf{u}_\infty &= (\mathbf{I} - \mathbf{Q} - \mathbf{LP})^{-1}(\mathbf{M}\mathbf{y}_d + \mathbf{L}\mathbf{d}_\infty) \end{aligned}$$

■

In order to have $\mathbf{e}_\infty = \mathbf{0}$, \mathbf{M} , \mathbf{L} and \mathbf{Q} should be selected as

$$\begin{aligned} \mathbf{Q} &= \mathbf{I} \\ \mathbf{M} &= -\mathbf{L} \end{aligned} \tag{4-22}$$

Proof:

From (4-20), for $\mathbf{e}_\infty = \mathbf{0}$, we should have

$$\begin{aligned} \mathbf{P}(\mathbf{I} - \mathbf{Q} - \mathbf{LP})^{-1}\mathbf{L} &= -\mathbf{I} \\ \mathbf{I} - \mathbf{Q} - \mathbf{LP} &= -\mathbf{LP} \\ \therefore \mathbf{Q} &= \mathbf{I} \end{aligned}$$

$$\begin{aligned} \mathbf{P}(\mathbf{I} - \mathbf{Q} - \mathbf{LP})^{-1}\mathbf{M} &= \mathbf{I} \\ \mathbf{I} - \mathbf{Q} - \mathbf{LP} &= \mathbf{MP} \\ \mathbf{I} - \mathbf{I} - \mathbf{LP} &= \mathbf{MP} \\ \therefore -\mathbf{L} &= \mathbf{M} \end{aligned}$$

■

Although the above matrices can achieve a zero asymptotic error, the transient error also needs to be analysed to prevent having significant transient errors in the system response. The controlled system is called monotonically convergent if

$$\|\mathbf{e}_\infty - \mathbf{e}_{k+1}\| \leq \gamma \|\mathbf{e}_\infty - \mathbf{e}_k\| \quad \forall k, 0 \leq \gamma < 1 \tag{4-23}$$

where $\|\cdot\|$ is the Euclidean norm, and γ is the convergence rate. For the ILC law given in (4-14) we have,

$$\gamma = \sigma\left(\frac{\mathbf{I} + \mathbf{LP}}{2}\right) \tag{4-24}$$

where $\sigma(\cdot)$ denotes the maximum singular value operator.

Proof:

$$\begin{aligned}
\mathbf{e}_\infty - \mathbf{e}_{k+1} &= (\mathbf{I} - \mathbf{P}(\mathbf{I} - \mathbf{Q} - \mathbf{LP})^{-1}\mathbf{M})\mathbf{y}_d - (\mathbf{P}(\mathbf{I} - \mathbf{Q} - \mathbf{LP})^{-1}\mathbf{L} + \mathbf{I})\mathbf{d}_\infty \\
&\quad - \mathbf{y}_d + \mathbf{P}(\mathbf{Q}\mathbf{u}_k + \mathbf{L}(\mathbf{P}\mathbf{u}_k + \mathbf{d}_k) + \mathbf{M}\mathbf{y}_d) + \mathbf{d}_{k+1} \\
&= (-\mathbf{P}(\mathbf{I} - \mathbf{Q} - \mathbf{LP})^{-1}\mathbf{M} + \mathbf{PM})\mathbf{y}_d + \mathbf{P}(\mathbf{Q} + \mathbf{LP})\mathbf{u}_k \\
&\quad - (\mathbf{P}(\mathbf{I} - \mathbf{Q} - \mathbf{LP})^{-1}\mathbf{L} + \mathbf{I})\mathbf{d}_\infty + \mathbf{PLd}_k + \mathbf{d}_{k+1}
\end{aligned}$$

Using values obtained in (4-22)

$$\mathbf{e}_\infty - \mathbf{e}_{k+1} = \mathbf{P}(\mathbf{I} + \mathbf{LP})\mathbf{u}_k - (\mathbf{I} + \mathbf{PL})\mathbf{y}_d + \mathbf{PLd}_k + \mathbf{d}_{k+1}$$

Also

$$\begin{aligned}
\mathbf{e}_\infty - \mathbf{e}_k &= (-\mathbf{P}(\mathbf{I} - \mathbf{Q} - \mathbf{LP})^{-1}\mathbf{M})\mathbf{y}_d + \mathbf{P}\mathbf{u}_k - (\mathbf{P}(\mathbf{I} - \mathbf{Q} - \mathbf{LP})^{-1}\mathbf{L} + \mathbf{I})\mathbf{d}_\infty + \mathbf{d}_k \\
&\quad - \mathbf{y}_d + \mathbf{P}\mathbf{u}_k + \mathbf{d}_k \\
&= (-\mathbf{P}(\mathbf{I} - \mathbf{Q} - \mathbf{LP})^{-1}\mathbf{M} - \mathbf{I})\mathbf{y}_d + 2\mathbf{P}\mathbf{u}_k - (\mathbf{P}(\mathbf{I} - \mathbf{Q} - \mathbf{LP})^{-1}\mathbf{L} + \mathbf{I})\mathbf{d}_\infty + 2\mathbf{d}_k
\end{aligned}$$

and by using values obtained in (4-22)

$$\mathbf{e}_\infty - \mathbf{e}_k = -2\mathbf{I}\mathbf{y}_d + 2\mathbf{P}\mathbf{u}_k + 2\mathbf{d}_k$$

Therefore,

$$\frac{\|\mathbf{e}_\infty - \mathbf{e}_{k+1}\|}{\|\mathbf{e}_\infty - \mathbf{e}_k\|} = \frac{\|-(\mathbf{I} + \mathbf{PL})\mathbf{y}_d + \mathbf{P}(\mathbf{I} + \mathbf{LP})\mathbf{u}_k + \mathbf{PLd}_k + \mathbf{d}_{k+1}\|}{\|-2\mathbf{I}\mathbf{y}_d + 2\mathbf{P}\mathbf{u}_k + 2\mathbf{d}_k\|}$$

Considering that in ILC $\{\mathbf{x}_k[0] = \mathbf{x}_0 \ \forall k\}$,

$$\mathbf{d}_k = \mathbf{d}_{k+1} = \mathbf{CA}^k \mathbf{x}_0 [\mathbf{1}]^T = \mathbf{d}$$

where $[\mathbf{1}]$ denotes an all one $1 \times N$ vector. Therefore,

$$\frac{\|\mathbf{e}_\infty - \mathbf{e}_{k+1}\|}{\|\mathbf{e}_\infty - \mathbf{e}_k\|} = \frac{\|-(\mathbf{I} + \mathbf{PL})\mathbf{y}_d + \mathbf{P}(\mathbf{I} + \mathbf{LP})\mathbf{u}_k + (\mathbf{I} + \mathbf{PL})\mathbf{d}\|}{\|-2\mathbf{I}\mathbf{y}_d + 2\mathbf{P}\mathbf{u}_k + 2\mathbf{d}\|}$$

Since for the matrices \mathbf{P} and \mathbf{L} given in (4-16) it can be proved that $\|(\mathbf{I} + \mathbf{PL})\| = \|(\mathbf{I} + \mathbf{LP})\|$, then

$$\frac{\|\mathbf{e}_\infty - \mathbf{e}_{k+1}\|}{\|\mathbf{e}_\infty - \mathbf{e}_k\|} \leq \frac{\|(\mathbf{I} + \mathbf{LP})\|}{2} \frac{\|-\mathbf{I}\mathbf{y}_d + \mathbf{P}\mathbf{u}_k + \mathbf{d}\|}{\|-\mathbf{I}\mathbf{y}_d + \mathbf{P}\mathbf{u}_k + \mathbf{d}\|}$$

$$\therefore \frac{\|\mathbf{e}_\infty - \mathbf{e}_{k+1}\|}{\|\mathbf{e}_\infty - \mathbf{e}_k\|} \leq \frac{\|(\mathbf{I} + \mathbf{LP})\|}{2} = \sigma\left(\frac{\mathbf{I} + \mathbf{LP}}{2}\right)$$

■

Using the results obtained from (4-19), (4-22) and (4-24), the ILC law given in (4-17) can achieve asymptotic stability as well as monotonic convergent and zero steady-state error when it is in the form of

$$\begin{aligned} \mathbf{u}_{k+1} &= \mathbf{u}_k + \mathbf{M}(\mathbf{y}_d - \mathbf{y}_k) \\ \rho(\mathbf{I} - \mathbf{MP}) &< 1 \\ \therefore 0 &\leq \sigma\left(\frac{\mathbf{I} - \mathbf{MP}}{2}\right) < 1 \end{aligned} \quad (4-25)$$

However, further consideration has to be taken into account before using (4-25) to control the pneumatic actuator. First, the considered pneumatic actuator is a nonlinear system with the state space equation of

$$\begin{cases} \dot{\mathbf{x}}_k(t) = f(\mathbf{x}_k(t), u_k(t)) \\ y_k(t) = g(\mathbf{x}_k(t)) \end{cases} ; t \in [0, T] \quad \mathbf{x}_k(0) = \mathbf{x}_0 \quad \forall k \quad (4-26)$$

We assume that $f : \mathbb{R}^{n+1} \rightarrow \mathbb{R}^n$ and $g : \mathbb{R}^{n+1} \rightarrow \mathbb{R}^1$ are global Lipschitz continuous (GLC) functions. Therefore,

$$\begin{aligned} \|f(\mathbf{x}_1, u_1, t) - f(\mathbf{x}_2, u_2, t)\| &\leq L_f(\|\mathbf{x}_1 - \mathbf{x}_2\| + \|u_1 - u_2\|) \\ \|g(\mathbf{x}_1, t) - g(\mathbf{x}_2, t)\| &\leq L_g\|\mathbf{x}_1 - \mathbf{x}_2\| \end{aligned} \quad (4-27)$$

Considering the estimated frequency of the pneumatic system obtained in the previous chapter, the system is asymptotically stable, and so for a sampling time of T_s , where $T = NT_s$, the system can be considered as

$$\begin{aligned} \mathbf{x}_k[i+1] &= \mathbf{A}\mathbf{x}_k[i] + \mathbf{B}u_k[i] + \xi(\mathbf{x}_k[i], u_k[i]) \\ y_k[i] &= \mathbf{C}\mathbf{x}_k[i] + \eta(\mathbf{x}_k[i]) \quad ; \quad \mathbf{x}_k[0] = \mathbf{x}_0 \quad \forall k, i \in [0, N] \end{aligned} \quad (4-28)$$

where $\lim_{\|\mathbf{x}\| \rightarrow 0} \frac{\|\xi\|}{\|\mathbf{x}\|} = 0$ and $\lim_{\|\mathbf{x}\| \rightarrow 0} \frac{\|\eta\|}{\|\mathbf{x}\|} = 0$. This means that the nonlinearities' effects in the system's dynamic would eventually vanish, and that the system has a dominating linear characteristic at its steady-state condition. Using (4-28), the system's output can be presented as

$$\begin{aligned} y_k[i] &= \mathbf{C}(q\mathbf{I} - \mathbf{A})^{-1} \mathbf{B} u_k[i] + \mathbf{C}\mathbf{A}^k \mathbf{x}_0 + \psi(u_k[i]) \\ &= P(q)u_k[i] + d_k + \psi(u_k[i]) \end{aligned} \quad (4-29)$$

where $\psi(\cdot)$ term is as a result of the nonlinearities' residue in the model. By applying the proposed ILC law given in (4-17), we have

$$\begin{aligned} \mathbf{u}_{k+1} &= \mathbf{Q}\mathbf{u}_k + \mathbf{L}\mathbf{y}_k + \mathbf{M}\mathbf{y}_d \\ &= (\mathbf{Q} + \mathbf{L}\mathbf{P})\mathbf{u}_k + (\mathbf{M}\mathbf{y}_d + \mathbf{L}\mathbf{d}_k) + \mathbf{L}\psi(\mathbf{u}_k) \end{aligned} \quad (4-30)$$

In order to make sure that the ILC method is AS, an additional term has been added to the ILC law as

$$\mathbf{u}_{k+1} = \mathbf{Q}\mathbf{u}_k + \mathbf{L}\mathbf{y}_k + \mathbf{M}\mathbf{y}_d - \alpha\mathbf{u}_k \quad (4-31)$$

where $\left\| \mathbf{L} \frac{\partial \psi}{\partial \mathbf{u}_k} \right\| \leq \alpha \quad \forall k$. The existence of α is guaranteed as $f(\cdot)$ and $g(\cdot)$ are assumed to be GLC functions.

As the nonlinearities in the system can be controlled (removed) by adding the proportional control term, $-\alpha\mathbf{u}_k$, the rest of the system can be considered linear, and (4-19), (4-22) and (4-24) will be held. Therefore, the ILC law for controlling the pneumatic actuator can be summarized as:

$$\begin{aligned} \mathbf{u}_{k+1} &= (1 - \alpha)\mathbf{u}_k + \mathbf{M}(\mathbf{y}_d - \mathbf{y}_k) \\ \rho(\mathbf{I} - \mathbf{MP}) &< 1 \\ 0 \leq \sigma\left(\frac{\mathbf{I} - \mathbf{MP}}{2}\right) &< 1 \end{aligned} \quad (4-32)$$

One major advantage of ILC is that it does not need accurate knowledge of the system model, and instead, it can learn from the system's historical input and output. However, some degree of estimation can help to obtain a better design with a faster convergence. For this purpose, the estimated bode plot, which was given in Figure 3.16, will be used. As is seen, the system is a lowpass with the bandwidth of 1.6rad/s. Therefore, we use

$$P(s) = \frac{0.01}{s + 1} \quad (4-33)$$

to estimate the linear part of the system. The ILC, in theory, is effective for repetitive processes. However, we would like to expand the ILC application to control the pneumatic system responding to non-repetitive inputs and disturbances. Since the system's bandwidth is 1.6rad/sec, it can be assumed that the system does not have much of fluctuations over a period of one second. Therefore, by taking $T = 0.01\text{s}$, we can consider that the system would be seen as a repetitive process from the controller's perspective. The $P(q)$ for the system given in (4-33) based on $T = 0.01\text{s}$ is equal to

$$P(q) = 9.95 \times 10^{-5} \times (q^{-1} + (0.99)q^{-2} + (0.99)^2q^{-3} + \dots) \quad (4-34)$$

and

$$\mathbf{P} = 9.95 \times 10^{-5} \times \begin{bmatrix} 1 & 0 & \dots & 0 \\ (0.99) & 1 & \ddots & 0 \\ \vdots & \vdots & \ddots & \vdots \\ (0.99)^{N-1} & (0.99)^{N-2} & \dots & 1 \end{bmatrix} \quad (4-35)$$

\mathbf{M} should be selected such that $\rho(\mathbf{I} - \mathbf{MP}) < 1$ and $0 \leq \sigma\left(\frac{\mathbf{I} - \mathbf{MP}}{2}\right) < 1$. Theoretically, $\mathbf{M} = \mathbf{P}^{-1}$ will perfectly satisfy both conditions. For $N = 10$, the inverse of \mathbf{P} is equal to

$$\mathbf{P}^{-1} = 1 \times 10^4 \times \begin{bmatrix} 1.005 & 0 & \dots & 0 \\ -0.995 & 1.005 & \dots & 0 \\ 0 & -0.995 & \ddots & \vdots \\ \vdots & \vdots & \dots & 1.005 \\ 0 & 0 & \dots & -0.995 \end{bmatrix} \quad (4-36)$$

However, this design causes discontinuities in the control loop and cannot be implemented. Nevertheless, as is seen from (4-36), $N = 2$ would be sufficient for implementing the ILC for the pneumatic actuator. Therefore, we consider \mathbf{M} as a 2×2 lower triangular matrix and calculate its arrays' values.

$$\mathbf{M} = \begin{bmatrix} m_0 & 0 \\ m_1 & m_0 \end{bmatrix} \quad \mathbf{P} = \begin{bmatrix} P_1 & 0 \\ P_2 & P_1 \end{bmatrix} \quad (4-37)$$

$$\mathbf{I} - \mathbf{MP} = \begin{bmatrix} 1 - m_0 P_1 & 0 \\ -m_0 P_2 - m_1 P_1 & 1 - m_0 P_1 \end{bmatrix}$$

$$\det(\lambda \mathbf{I} - (\mathbf{I} - \mathbf{MP})) = \det \begin{pmatrix} \lambda - 1 + m_0 P_1 & 0 \\ m_0 P_2 + m_1 P_1 & \lambda - 1 + m_0 P_1 \end{pmatrix} = 0$$

$$\lambda = 1 - m_0 P_1$$

$$\rho(\mathbf{I} - \mathbf{MP}) = 1 - m_0 P_1$$

$$\therefore 0 \leq m_0 \leq \frac{1}{P_1} = 10050$$

$$\sigma \left(\frac{\mathbf{I} - \mathbf{MP}}{2} \right) = \frac{\|\mathbf{I} - \mathbf{MP}\|}{2} = \frac{\sqrt{2(1 - m_0 P_1)^2 + (m_0 P_2 + m_1 P_1)^2}}{2}$$

$$\therefore \frac{-m_0 P_2 - \sqrt{4 - 2(1 - m_0 P_1)^2}}{P_1} \leq m_1 \leq \frac{\sqrt{4 - 2(1 - m_0 P_1)^2} - m_0 P_2}{P_1}$$

Although from the theoretical perspective, a larger value of m_0 improves the AS condition of the ILC method, from the practical aspect, it should be limited to prevent the system from saturation. Considering the maximum rod's displacement as 0.2m and the maximum input

voltage as 12V, the maximum value of m_0 should be limited to $m_0 \leq \frac{12}{0.2} = 60$. Figure 4.9 shows the relation between $\sigma\left(\frac{I-MP}{2}\right)$ and $m_1 \in [-60,60]$ to prevent the system from being saturated. For a repetitive process perspective, the best value would be $m_1 = -60$ to minimize the transient error as is given by (4-24). However, the inputs to the considered pneumatic system are not repetitive, and so the proof given for (4-24) has to be revisited. As part of this proof we had

$$\frac{\|e_\infty - e_{k+1}\|}{\|e_\infty - e_k\|} = \frac{\|-(I + PL)y_d + P(I + LP)u_k + PLd_k + d_{k+1}\|}{\|-2Iy_d + 2Pu_k + 2d_k\|} \quad (4-38)$$

However, as the process is not repetitive, we cannot consider $d_k = d_{k+1}$. Instead, we should select the PL value as its maximum value, since this choice can help the condition to be asymptotically held as $\lim_{PL \rightarrow \infty} \left\{ \frac{PLd_k + d_{k+1}}{PLd_k + d_k} \right\} = 1$. Therefore, the values in (4-37) are selected as $m_0 = m_1 = 60$, which makes $\rho = 0.994$ and $\sigma = 0.5$, satisfying the conditions in (4-32). The value for α should be in the range of $[0,1)$ to satisfy the AS condition of the ILC method. However, choosing the optimal value requires the system's knowledge, which is not available. Therefore, we performed a set of experiments and found that $\alpha = 0.25$ can lead to satisfactory performance.

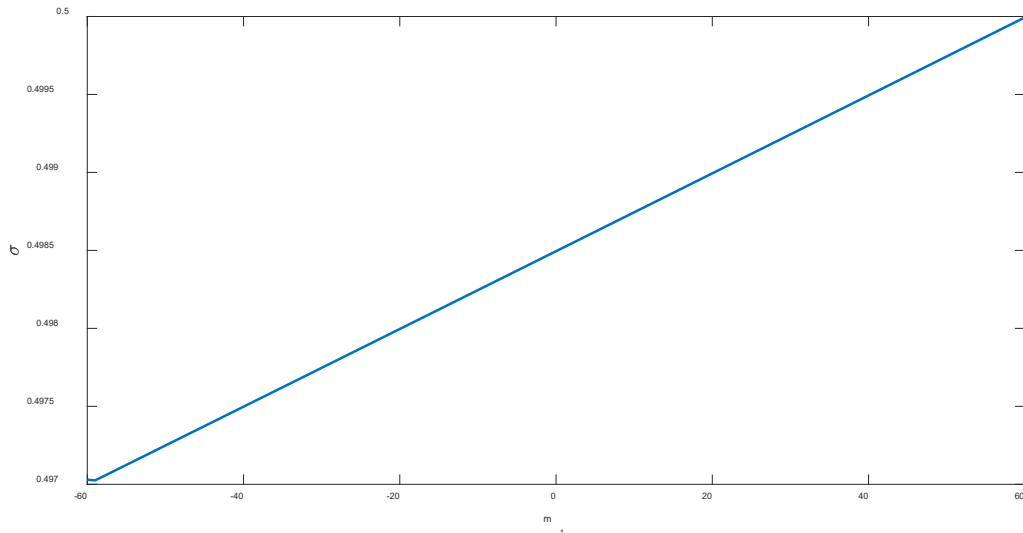


Figure 4.9. The effect of learning function value on the σ

Based on the above discussions, the designed ILC method for the pneumatic actuator system is implemented as

$$u_{k+1}[n] = 0.75u_k[n] + (60 + 60q^{-1})(y_d[n] - y_k[n]) \tag{4-39}$$

The performance of the ILC-controlled system in tracking a reference signal is shown in Figure 4.10, and is compared to the performance of the PID controller in Figure 4.11, which shows a faster and more accurate response.

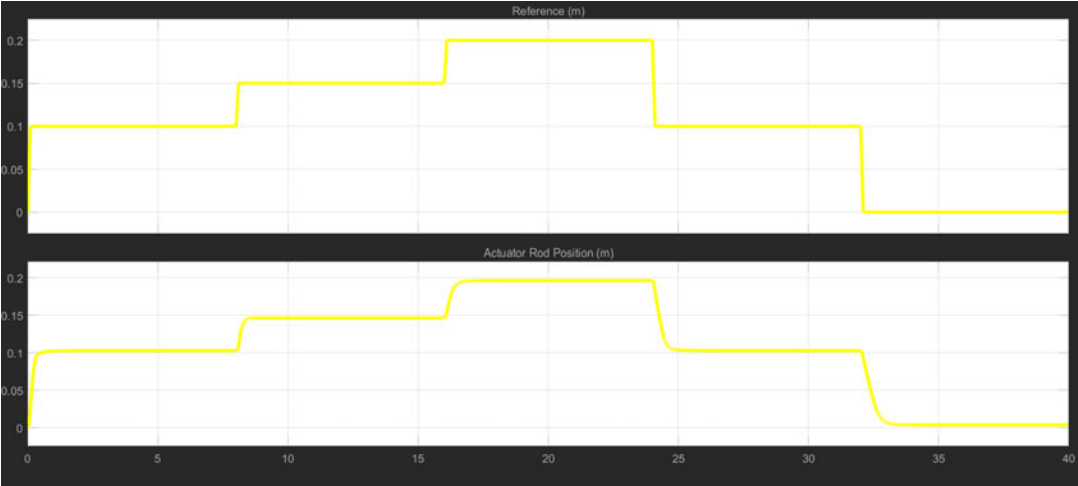


Figure 4.10. Tracking performance of the ILC controlled actuator

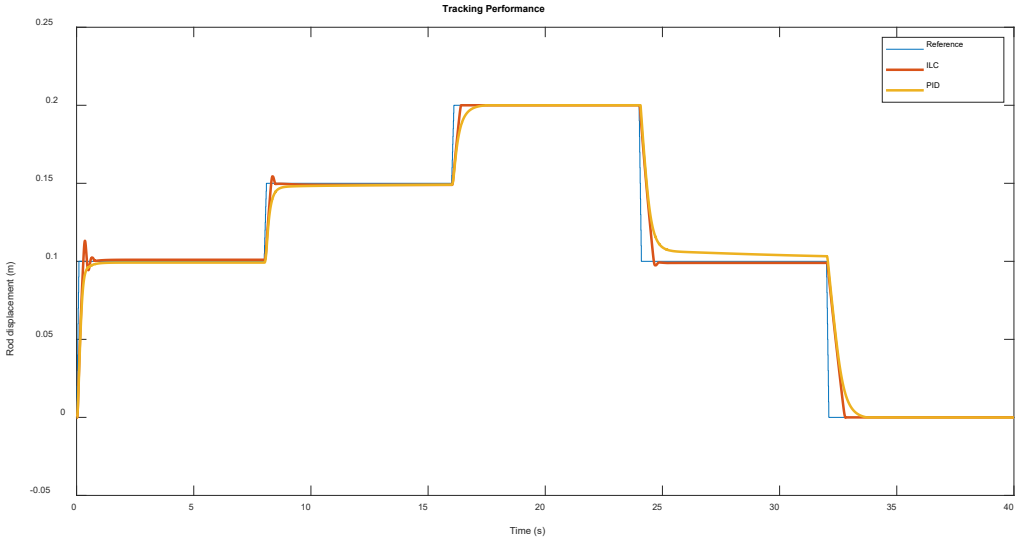


Figure 4.11. The comparison between the ILC and PID performance in tracking a reference signal

The difference between the reference and output of the system controlled by the ILC and PID is shown in Figure 4.12. As is seen, the tracking requirement has been achieved at the steady-state. The ILC can obtain the $\pm 0.002\text{m}$ precision in 0.56s compared to 0.75s for the PID. The summation of the square of the error ($\int e^2(t)dt$) for the PID controller is 0.0055 , whereas this for the ILC controller is 0.0044 . Therefore, the ILC demonstrates superior performance than the PID controller in terms of both speed and tracking accuracy.

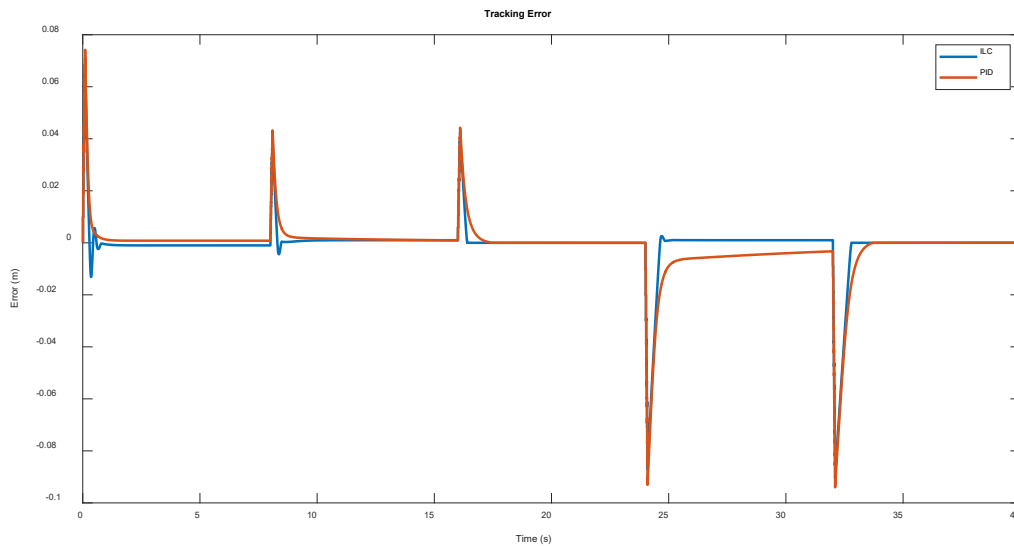


Figure 4.12. Comparison of PID and ILC with respect to the tracking error

Next, we investigate the performance of the ILC method to overcome uncertainties. The performance of the system in overcoming the payload uncertainty is demonstrated in Figure 4.13, showing that the controller can maintain the required precision ($\pm 0.002\text{m}$) regardless of changes in the load. Although PID could not respond adequately to the uncertainties, the performance of the ILC and PID controllers in responding to the payload uncertainty is depicted in Figure 4.14. The summation of the square of the error for the PID controller is 9.1×10^{-4} , whereas this for the ILC controller is 3.4×10^{-4} . Again, the ILC shows a better performance than the PID controller in overcoming the uncertainties.

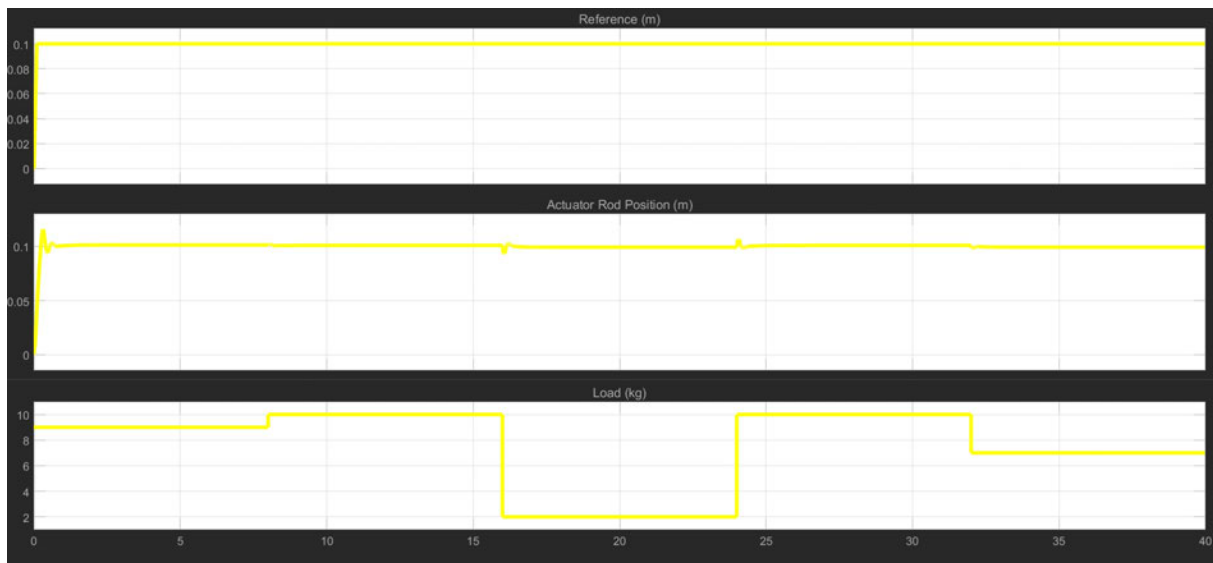


Figure 4.13. Performance of the ILC controlled actuator under payload uncertainty

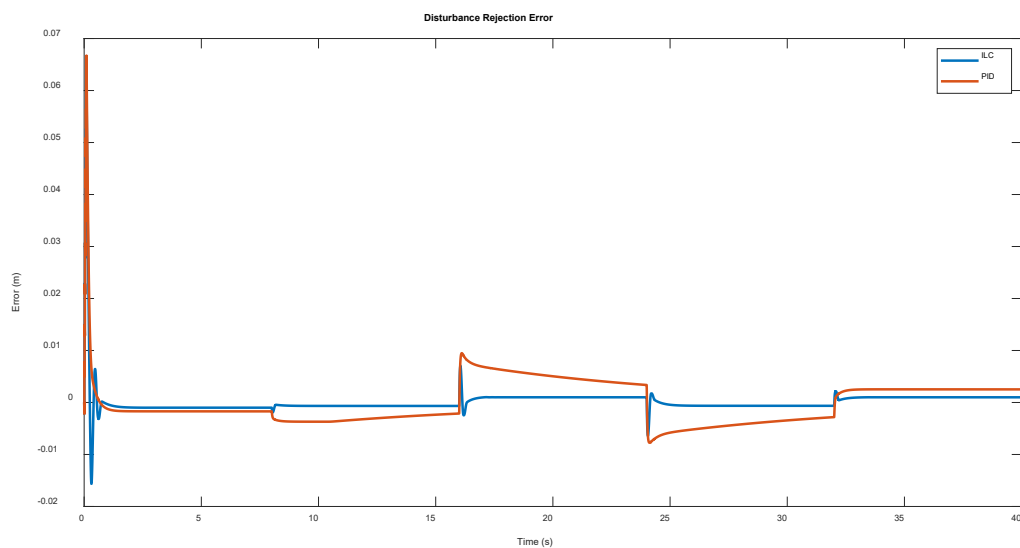


Figure 4.14. Comparison of PID and ILC with respect to overcoming payload uncertainty

4.5. Summary

This chapter covered the procedure for designing an ILC controller for the considered pneumatic actuator. It was shown through theoretical analysis that the ILC is a model-free

controller, which means no prior knowledge of the system model is required during the design procedure. The whole design was done based on the information obtained from the input and output of the system. We further expand the ILC method in order to be applicable to nonlinear, non-repetitive systems so that it can be used to control the considered pneumatic system. The performance of the ILC-controlled system was compared with a well-tuned PID controller. For this purpose, a PID controller has been designed based on the estimated frequency response of the plant. The simulation results showed that the designed ILC controller was successfully capable of tracking a non-repetitive reference signal and could overcome the internal and payload uncertainties. With respect to speed, the ILC was also shown to have better performance compared to the PID controller.

CHAPTER 5: CONCLUSION

Cylinder-piston actuators are the most common pneumatic systems, which translate the air pressure force into a linear mechanical motion. In industrial automation and robotics, linear pneumatic actuators have a wide range of applications, from load positioning to pneumatic muscles in robots. The air is, however, compressible and has a low damping characteristic, which causes a nonlinear response and increases the system's dynamic order. Moreover, before the system can apply any force to a load, a pneumatic system's pipes and cylinders have to be filled with air. This results in further nonlinearities in the form of dead-band and transmission attenuations. Also, a pneumatic system is affected by frictional forces caused by the mechanical parts' movements. Such nonlinearities make identifying pneumatic systems' parameters, which are needed by many control algorithms to precisely control the system's position, a challenging practice.

The methods of controlling pneumatic actuators were reviewed in Chapter 2, where they were classified into PID-based, robust methods, adaptive methods and intelligent based controllers. It was discussed that the main challenge in controlling pneumatic actuators is to overcome the nonlinearities and uncertainties of the system. Two approaches have been taken for designing controllers for pneumatic systems. In the first approach, as is done in robust control methods, uncertainty boundaries are identified and the controller is designed within those boundaries. In the second approach, the controllers are capable of being adjusted to the system's variations. However, this requires continuously estimating the system's parameters using measurements, as is done in adaptive controllers, or performing extensive calculations and training as in intelligent based methods. A well-tuned PID controller can also achieve the required performance. The tuning can be done by the designer or by the system itself using different adaptive and intelligent methods.

In the majority of the control algorithms used in controlling the position of a pneumatic actuator, the model of the system has to be achieved prior to the design of the controller. However, due to the gases' physical behaviour, modelling a pneumatic system is usually done based on many assumptions that might result in an inaccurate model during system operation. As a result, such controllers may not achieve the required performance. Moreover, intelligent based control algorithms cannot easily be implemented in real-time applications due to their

extensive calculation requirements. This leads to a need for developing real-time control systems capable of controlling pneumatic systems without needing to obtain the mathematical model of the system.

An ILC algorithm uses information from previous repetitions to learn about the system's dynamics for generating a more suitable control signal. This learning process is performed in an iterative manner to improve the controller's performance from one iteration to the other, achieving a zero-error convergence. ILC algorithms are particularly useful in real-time control systems, given their relatively quick response to changes in the input signal. However, their application is only limited to repetitive processes, where the same control action should be performed repeatedly. In such processes, it is reasonable to make use of previously acquired data for improving a controller's convergence and robustness. Therefore, the aim of this study was to design an ILC controller for position control of a pneumatic system to achieve $\pm 2\text{mm}$ precision in controlling the position of 1-10 kg payloads. Such a performance has been selected based on the industrial applications of approximately 70% of servo pneumatic actuators.

Although ILC is a model-free control method, in Chapter 3, the mathematical model and physical properties of a pneumatic actuator have been discussed. This was to provide a better understanding of the nonlinearities and uncertainties that have been considered in modelling the selected pneumatic system. The modelling has been done according to theoretical analysis, including thermodynamics, fluid mechanics and motion dynamics theories. In addition to the mathematical model derivation, Chapter 3 covered the simulation of the system using MATLAB SimScape. The simulation results have demonstrated the effect of system nonlinearities on the system's response.

Chapter 4 discussed the procedure for designing a well-tuned PID and an ILC controller for the considered pneumatic actuator to be able to compare their performances. The frequency domain techniques, namely Nichols chart and Inverse Nichols chart, have been used to design the PID controller. Although the PID-controlled system performed adequately in reference tracking, it was unsuccessful in overcoming the payload uncertainties. It was then shown through theoretical analysis that the ILC is a model-free controller, which means no prior knowledge of the system model is required during the design procedure. The whole design was done based on the information obtained from the input and output of the system. The ILC

method has been even further expanded to be applicable to nonlinear, non-repetitive systems so that it could be used to control the considered pneumatic system. This was done through detailed mathematical analysis of the system. The simulation results showed that the designed ILC controller was successfully capable of tracking a non-repetitive reference signal and could overcome the internal and payload uncertainties. With respect to speed, the ILC was also shown to have better performance compared to the PID controller.

REFERENCES

- [1] A. Tootchi and A. Chaibakhsh, "Fault Tolerant Control for Trajectory Tracking of a Pneumatic Servo Positioning System," in *2018 6th RSI International Conference on Robotics and Mechatronics (IcRoM)*, 2018: IEEE, pp. 53-58.
- [2] N. A. Markov, I. A. Shipitko, and T. V. Bezruchko, "Synthesis of the Position Controller for the Pneumatic Actuator," in *2009 International Siberian Conference on Control and Communications*, 2009: IEEE, pp. 116-120.
- [3] R. B. Van Varseveld and G. M. Bone, "Accurate Position Control of a Pneumatic Actuator Using on/Off Solenoid Valves," *IEEE/ASME Transactions on mechatronics*, vol. 2, no. 3, pp. 195-204, 1997.
- [4] R. Rosli, M. Mailah, and G. Priyandoko, "Active Suspension System for Passenger Vehicle Using Active Force Control with Iterative Learning Algorithm," *WSEAS Trans. Syst. Control*, vol. 9, pp. 120-129, 2014.
- [5] F. Bu and H.-S. Tan, "Pneumatic Brake Control for Precision Stopping of Heavy-Duty Vehicles," *IEEE Transactions on Control Systems Technology*, vol. 15, no. 1, pp. 53-64, 2006.
- [6] S. Kadam, V. Gaikwad, H. Bhavsar, and S. Kulkarni, "Electro-Pneumatic Lift and Carry Conveying System," *International Journal of Science Technology & Engineering*, vol. 2, no. 10, 2016.
- [7] M. Rahmat, N. Kamaruddin, and M. Isa, "Flow Regime Identification in Pneumatic Conveyor Using Electrodynamic Transducer and Fuzzy Logic Method," *International Journal on Smart Sensing and Intelligent Systems*, vol. 2, no. 3, 2017.
- [8] S. Balasubramanian, H. Huang, and H. Jiping, "Quantification of Dynamic Property of Pneumatic Muscle Actuator for Design of Therapeutic Robot Control. Engineering in Medicine and Biology Society," in *EMBS'06. 28th Annual International Conference of the IEEE, IEEE*, 2006.
- [9] J. Schröder, K. Kawamura, T. Gockel, and R. Dillmann, "Improved Control of a Humanoid Arm Driven by Pneumatic Actuators," *Proceedings of Humanoids 2003*, 2003.
- [10] B. Yao, Z. Zhou, Q. Liu, and Q. Ai, "Empirical Modeling and Position Control of Single Pneumatic Artificial Muscle," *Journal of Control Engineering and Applied Informatics*, vol. 18, no. 2, pp. 86-94, 2016.
- [11] B. Taheri, D. Case, and E. Richer, "Design of Robust Nonlinear Force and Stiffness Controller for Pneumatic Actuators," in *2012 IEEE 51st IEEE Conference on Decision and Control (CDC)*, 2012: IEEE, pp. 1192-1198.
- [12] S.-C. Hsu and C.-Y. Lin, "Periodic Motion Control of a Heavy Duty Pneumatic Actuating Table Using Low-Cost Position Sensors and Hybrid Repetitive Control," in *2013 IEEE International Symposium on Industrial Electronics*, 2013: IEEE, pp. 1-6.
- [13] G. M. Bone, M. Xue, and J. Flett, "Position Control of Hybrid Pneumatic-Electric Actuators Using Discrete-Valued Model-Predictive Control," *Mechatronics*, vol. 25, pp. 1-10, 2015.
- [14] K. Hamiti, A. Voda-Besancon, and H. Roux-Buisson, "Position Control of a Pneumatic Actuator under the Influence of Stiction," *Control Engineering Practice*, vol. 4, no. 8, pp. 1079-1088, 1996.
- [15] R. Weston, P. Moore, T. Thatcher, and G. Morgan, "Computer Controlled Pneumatic Servo Drives," *Proceedings of the Institution of Mechanical Engineers, Part B: Management and engineering manufacture*, vol. 198, no. 4, pp. 275-281, 1984.
- [16] R. Nagarajan and R. Weston, "Front End Control Schemes for Pneumatic Servo-Driven Modules," *Proceedings of the Institution of Mechanical Engineers, Part B: Management and engineering manufacture*, vol. 199, no. 4, pp. 271-277, 1985.
- [17] S. Kobayashi, M. Cotsaftis, and T. Takamori, "Robust Control of Pneumatic Actuators Based on Dynamic Impedance Matching," in *1995 IEEE International Conference on*

- Systems, Man and Cybernetics. Intelligent Systems for the 21st Century*, 1995, vol. 2: IEEE, pp. 983-987.
- [18] S. Jamian *et al.*, "Review on Controller Design in Pneumatic Actuator Drive System," *Telkomnika*, vol. 18, no. 1, pp. 332-342, 2020.
- [19] H. Morioka, A. Nishiuchi, K. Kurahara, K. Tanaka, and M. Oka, "Practical Robust Control Design of Pneumatic Servo Systems," in *2000 26th Annual Conference of the IEEE Industrial Electronics Society. IECON 2000. 2000 IEEE International Conference on Industrial Electronics, Control and Instrumentation. 21st Century Technologies*, 2000, vol. 3: IEEE, pp. 1755-1760.
- [20] J. Wang, J. Pu, and P. Moore, "Accurate Position Control of Servo Pneumatic Actuator Systems: An Application to Food Packaging," *Control Engineering Practice*, vol. 7, no. 6, pp. 699-706, 1999.
- [21] A. Saleem, C.-B. Wong, J. Pu, and P. R. Moore, "Mixed-Reality Environment for Frictional Parameters Identification in Servo-Pneumatic System," *Simulation Modelling Practice and Theory*, vol. 17, no. 10, pp. 1575-1586, 2009.
- [22] J. Wang, J. Pu, and P. Moore, "A Practical Control Strategy for Servo-Pneumatic Actuator Systems," *Control Engineering Practice*, vol. 7, no. 12, pp. 1483-1488, 1999.
- [23] A. Ilchmann, O. Sawodny, and S. Trenn, "Pneumatic Cylinders: Modelling and Feedback Force-Control," *International Journal of Control*, vol. 79, no. 06, pp. 650-661, 2006.
- [24] M. Papoutsidakis, G. Gkafas, S. Kanavetas, and G. Chamilothoris, "Modeling and Simulated Control of Non-Linear Switching Actuation Systems," in *Proceedings of the 8th WSEAS international conference on System science and simulation in engineering, Genova, Italy*, 2009.
- [25] W. Lai, M. Rahmat, and N. A. Wahab, "Modeling and Controller Design of Pneumatic Actuator System with Control Valve," *International Journal on Smart Sensing & Intelligent Systems*, vol. 5, no. 3, 2012.
- [26] A. a. M. Faudzi, K. Bin Osman, M. Rahmat, M. A. Azman, and K. Suzumori, "Controller Design for Simulation Control of Intelligent Pneumatic Actuators (Ipa) System," *Procedia Engineering*, vol. 41, pp. 593-599, 2012.
- [27] N. Sunar, M. Rahmat, Z. H. Ismail, A. a. M. Faudzi, and S. N. S. Salim, "Model Identification and Controller Design for an Electro-Pneumatic Actuator System with Dead Zone Compensation," *International Journal on Smart Sensing and Intelligent Systems*, vol. 7, no. 2, 2017.
- [28] H. K. Lee, G. S. Choi, and G. H. Choi, "A Study on Tracking Position Control of Pneumatic Actuators," *Mechatronics*, vol. 12, no. 6, pp. 813-831, 2002.
- [29] A. Saleem, B. Taha, T. Tutunji, and A. Al-Qaisia, "Identification and Cascade Control of Servo-Pneumatic System Using Particle Swarm Optimization," *Simulation Modelling Practice and Theory*, vol. 52, pp. 164-179, 2015.
- [30] Y.-S. Jeon, C.-O. Lee, and Y.-S. Hong, "Optimization of the Control Parameters of a Pneumatic Servo Cylinder Drive Using Genetic Algorithms," *Control Engineering Practice*, vol. 6, no. 7, pp. 847-853, 1998.
- [31] H.-P. Ren, J.-T. Fan, and O. Kaynak, "Optimal Design of a Fractional-Order Proportional-Integer-Differential Controller for a Pneumatic Position Servo System," *IEEE Transactions on Industrial Electronics*, vol. 66, no. 8, pp. 6220-6229, 2018.
- [32] W.-D. Chang, R.-C. Hwang, and J.-G. Hsieh, "A Self-Tuning Pid Control for a Class of Nonlinear Systems Based on the Lyapunov Approach," *Journal of Process Control*, vol. 12, no. 2, pp. 233-242, 2002.
- [33] S. N. Syed Salim, M. F. A. Rahmat, M. Faudzi, Z. H. Ismail, and N. Sunar, "Position Control of Pneumatic Actuator Using Self-Regulation Nonlinear Pid," *Mathematical Problems in Engineering*, vol. 2014, 2014.
- [34] M. Rahmat, S. N. S. Salim, N. Sunar, A. M. Faudzi, Z. H. Ismail, and K. Huda, "Identification and Non-Linear Control Strategy for Industrial Pneumatic Actuator," *International Journal of Physical Sciences*, vol. 7, no. 17, pp. 2565-2579, 2012.
- [35] S. N. S. Salim, M. Rahmat, A. a. M. Faudzi, and Z. H. Ismail, "Position Control of Pneumatic Actuator Using an Enhancement of Npid Controller Based on the

- Characteristic of Rate Variation Nonlinear Gain," *The International Journal of Advanced Manufacturing Technology*, vol. 75, no. 1-4, pp. 181-195, 2014.
- [36] S. N. S. Salim *et al.*, "A Study on Tracking Performance of the Pneumatic System with Enhanced Npid Controller," in *2015 10th Asian Control Conference (ASCC)*, 2015: IEEE, pp. 1-6.
- [37] J. Wang, Ü. Kotta, and J. Ke, "Tracking Control of Nonlinear Pneumatic Actuator Systems Using Static State Feedback Linearization of the Input-Output Map," in *Proceedings of the Estonian Academy of Sciences, Physics, Mathematics*, 2007, vol. 56, no. 1.
- [38] K. Karim, B. Pascal, and A. Louis, "Force Control Loop Affected by Bounded Uncertainties and Unbounded Inputs for Pneumatic Actuator Systems, Asme," *Journal of Dynamic Systems, Measurement, and Control*, vol. 130, pp. 1-9, 2008.
- [39] K. Khayati, P. Bigras, and L.-A. Dessaint, "A Robust Feedback Linearization Force Control of a Pneumatic Actuator," in *2004 IEEE International Conference on Systems, Man and Cybernetics (IEEE Cat. No. 04CH37583)*, 2004, vol. 7: IEEE, pp. 6113-6119.
- [40] M. Karpenko and N. Sepehri, "Qft Design of a Pi Controller with Dynamic Pressure Feedback for Positioning a Pneumatic Actuator," in *Proceedings of the 2004 American Control Conference*, 2004, vol. 6: IEEE, pp. 5084-5089.
- [41] M. Karpenko and N. Sepehri, "Qft Synthesis of a Position Controller for a Pneumatic Actuator in the Presence of Worst-Case Persistent Disturbances," in *2006 American Control Conference*, 2006: IEEE, p. 6 pp.
- [42] J. Song and Y. Ishida, "A Robust Sliding Mode Control for Pneumatic Servo Systems," *International journal of engineering science*, vol. 35, no. 8, pp. 711-723, 1997.
- [43] E. Richer and Y. Hurmuzlu, "A High Performance Pneumatic Force Actuator System: Part I—Nonlinear Mathematical Model," *J. dyn. sys., meas., control*, vol. 122, no. 3, pp. 416-425, 2000.
- [44] M. Smaoui, X. Brun, and D. Thomasset, "Systematic Control of an Electropneumatic System: Integrator Backstepping and Sliding Mode Control," *IEEE transactions on control systems technology*, vol. 14, no. 5, pp. 905-913, 2006.
- [45] G. M. Bone and S. Ning, "Experimental Comparison of Position Tracking Control Algorithms for Pneumatic Cylinder Actuators," *IEEE/ASME Transactions on mechatronics*, vol. 12, no. 5, pp. 557-561, 2007.
- [46] Y.-C. Tsai and A.-C. Huang, "Multiple-Surface Sliding Controller Design for Pneumatic Servo Systems," *Mechatronics*, vol. 18, no. 9, pp. 506-512, 2008.
- [47] S. Hodgson, M. Q. Le, M. Tavakoli, and M. T. Pham, "Sliding-Mode Control of Nonlinear Discrete-Input Pneumatic Actuators," in *2011 IEEE/RSJ International Conference on Intelligent Robots and Systems*, 2011: IEEE, pp. 738-743.
- [48] A. Estrada and F. Plestan, "Second Order Sliding Mode Output Feedback Control with Switching Gains—Application to the Control of a Pneumatic Actuator," *Journal of the Franklin Institute*, vol. 351, no. 4, pp. 2335-2355, 2014.
- [49] M. C. Hidalgo and C. Garcia, "Friction Compensation in Control Valves: Nonlinear Control and Usual Approaches," *Control Engineering Practice*, vol. 58, pp. 42-53, 2017.
- [50] Y.-C. Tsai and A.-C. Huang, "Fat-Based Adaptive Control for Pneumatic Servo Systems with Mismatched Uncertainties," *Mechanical Systems and Signal Processing*, vol. 22, no. 6, pp. 1263-1273, 2008.
- [51] Y. Shtessel, F. Plestan, and M. Taleb, "Lyapunov Design of Adaptive Super-Twisting Controller Applied to a Pneumatic Actuator," *IFAC Proceedings Volumes*, vol. 44, no. 1, pp. 3051-3056, 2011.
- [52] Y. Zhu and E. J. Barth, "Accurate Sub-Millimeter Servo-Pneumatic Tracking Using Model Reference Adaptive Control (Mrac)," *International Journal of Fluid Power*, vol. 11, no. 2, pp. 43-55, 2010.
- [53] M. Farag and N. Z. Azlan, "Adaptive Backstepping Position Control of Pneumatic Anthropomorphic Robotic Hand," *Procedia Computer Science*, vol. 76, pp. 161-167, 2015.

- [54] S. Kaitwanidvilai and M. Parnichkun, "Force Control in a Pneumatic System Using Hybrid Adaptive Neuro-Fuzzy Model Reference Control," *Mechatronics*, vol. 15, no. 1, pp. 23-41, 2005.
- [55] S. Alexandru, P. Gheorghe, and C. Bogdan, "Aspects Regarding the Neuroadaptive Control Structure Properties Application to the Nonlinear Pneumatic Servo System Benchmark, Electrotechnics," *Electronics, Automatic Control, Informatics*, pp. 82-86, 2006.
- [56] M. Yamazaki and S. Yasunobu, "An Intelligent Control for State-Dependent Nonlinear Actuator and Its Application to Pneumatic Servo System," in *SICE Annual Conference 2007*, 2007: IEEE, pp. 2194-2199.
- [57] B. Najjari, S. M. Barakati, A. Mohammadi, M. J. Futohi, and M. Bostanian, "Position Control of an Electro-Pneumatic System Based on Pwm Technique and Flc," *ISA transactions*, vol. 53, no. 2, pp. 647-657, 2014.
- [58] M. P. S. Dos Santos and J. Ferreira, "Novel Intelligent Real-Time Position Tracking System Using Fpga and Fuzzy Logic," *Isa Transactions*, vol. 53, no. 2, pp. 402-414, 2014.
- [59] D. Saravanakumar and B. Mohan, "Fuzzy Based Control System for Interconnected Pneumatic Cylinder Linear Positioning System," in *Applied Mechanics and Materials*, 2014, vol. 592: Trans Tech Publ, pp. 2145-2149.
- [60] D. Saravanakumar, B. Mohan, and T. Muthuramalingam, "Optimization of Proportional Fuzzy Controller for Servo Pneumatic Positioning System Using Taguchi: Data Envelopment Analysis Based Ranking Methodology," *Journal of Engineering and Technology*, vol. 4, no. 2, 2014.
- [61] X. Wang and G. Peng, "Modeling and Control for Pneumatic Manipulator Based on Dynamic Neural Network," in *SMC'03 Conference Proceedings. 2003 IEEE International Conference on Systems, Man and Cybernetics. Conference Theme-System Security and Assurance (Cat. No. 03CH37483)*, 2003, vol. 3: IEEE, pp. 2231-2236.
- [62] Q. Song and F. Liu, "Neural Network Modeling and Disturbance Observer Based Control of a Pneumatic System," in *2006 2nd IEEE/ASME International Conference on Mechatronics and Embedded Systems and Applications*, 2006: IEEE, pp. 1-5.
- [63] K. K. Ahn and H. T. C. Nguyen, "Intelligent Switching Control of a Pneumatic Muscle Robot Arm Using Learning Vector Quantization Neural Network," *Mechatronics*, vol. 17, no. 4-5, pp. 255-262, 2007.
- [64] Q. Song, F. Liu, and R. D. Findlay, "Improved Fuzzy Neural Network Control for a Pneumatic System Based on Extended Kalman Filter," in *2006 International Conference on Computational Intelligence for Modelling Control and Automation and International Conference on Intelligent Agents Web Technologies and International Commerce (CIMCA'06)*, 2006: IEEE, pp. 76-76.
- [65] N. N. Son, C. Van Kien, and H. P. H. Anh, "A Novel Adaptive Feed-Forward-Pid Controller of a Scara Parallel Robot Using Pneumatic Artificial Muscle Actuator Based on Neural Network and Modified Differential Evolution Algorithm," *Robotics and Autonomous Systems*, vol. 96, pp. 65-80, 2017.
- [66] J. E. Takosoglu, R. F. Dindorf, and P. A. Laski, "Rapid Prototyping of Fuzzy Controller Pneumatic Servo-System," *The International Journal of Advanced Manufacturing Technology*, vol. 40, no. 3, pp. 349-361, 2009.
- [67] X. Gao and Z.-J. Feng, "Design Study of an Adaptive Fuzzy-Pd Controller for Pneumatic Servo System," *Control Engineering Practice*, vol. 13, no. 1, pp. 55-65, 2005.
- [68] J. E. Takosoglu, P. A. Laski, and S. Blasiak, "A Fuzzy Logic Controller for the Positioning Control of an Electro-Pneumatic Servo-Drive," *Proceedings of the Institution of Mechanical Engineers, Part I: Journal of Systems and Control Engineering*, vol. 226, no. 10, pp. 1335-1343, 2012.
- [69] Z. Haiyan, S. Lepeng, and D. Zhiming, "Valve Barrel Position Control Based on Self-Tuning Fuzzy Pid with Particle Swarm Optimization," *International Journal on Smart Sensing & Intelligent Systems*, vol. 9, no. 3, 2016.

- [70] O. F. Hikmat, M. O. Elnimair, and K. Osman, "Pi Adaptive Neuro-Fuzzy and Receding Horizon Position Control for Intelligent Pneumatic Actuator," *Jurnal Teknologi*, vol. 67, no. 3, 2014.
- [71] A. Irawan and M. I. P. Azahar, "Cascade Control Strategy on Servo Pneumatic System with Fuzzy Self-Adaptive System," *Journal of Control, Automation and Electrical Systems*, pp. 1-14, 2020.
- [72] B. Dehghan, S. Taghizadeh, B. Surgenor, and M. Abu-Mallouh, "A Novel Adaptive Neural Network Compensator as Applied to Position Control of a Pneumatic System," *Intelligent Control and Automation*, vol. 2, no. 04, p. 388, 2011.
- [73] C.-K. Chen and J. Hwang, "Iterative Learning Control for Position Tracking of a Pneumatic Actuated Xy Table," in *Proceedings of the 2004 IEEE International Conference on Control Applications, 2004.*, 2004, vol. 1: IEEE, pp. 388-393.
- [74] S. Yu, J. Bai, S. Xiong, and R. Han, "A New Iterative Learning Controller for Electro-Pneumatic Servo System," in *2008 eighth international conference on intelligent systems design and applications*, 2008, vol. 3: IEEE, pp. 101-105.
- [75] K. Qian, Z. Li, A. Asker, Z. Zhang, and S. Xie, "Robust Iterative Learning Control for Pneumatic Muscle with State Constraint and Model Uncertainty," in *2021 IEEE International Conference on Robotics and Automation (ICRA)*, 2021: IEEE, pp. 5980-5987.
- [76] Q. Ai *et al.*, "High-Order Model-Free Adaptive Iterative Learning Control of Pneumatic Artificial Muscle with Enhanced Convergence," *IEEE Transactions on Industrial Electronics*, vol. 67, no. 11, pp. 9548-9559, 2019.
- [77] J. Rwafa and F. Ghayoor, "Implementation of Iterative Learning Control on a Pneumatic Control Valve," in *2019 International Multidisciplinary Information Technology and Engineering Conference (IMITEC)*, 2019: IEEE, pp. 1-5.
- [78] S. Arimoto, S. Kawamura, and F. Miyazaki, "Bettering Operation of Robots by Learning," *Journal of Robotic systems*, vol. 1, no. 2, pp. 123-140, 1984.
- [79] M. Garden, "Learning Control of Actuators in Control Systems," ed: Google Patents, 1971.
- [80] M. Uchiyama, "Formation of High-Speed Motion Pattern of a Mechanical Arm by Trial," *Transactions of the Society of Instrument and Control Engineers*, vol. 14, no. 6, pp. 706-712, 1978.
- [81] K. L. Moore, "Iterative Learning Control for Deterministic Systems," 2012.
- [82] K. J. Hunt, D. Sbarbaro, R. Żbikowski, and P. J. Gawthrop, "Neural Networks for Control Systems—a Survey," *Automatica*, vol. 28, no. 6, pp. 1083-1112, 1992.
- [83] N. Amann, D. H. Owens, and E. Rogers, "Iterative Learning Control for Discrete-Time Systems with Exponential Rate of Convergence," *IEE Proceedings-Control Theory and Applications*, vol. 143, no. 2, pp. 217-224, 1996.
- [84] G. Hillerström and K. Walgama, "Repetitive Control Theory and Applications-a Survey," *IFAC Proceedings Volumes*, vol. 29, no. 1, pp. 1446-1451, 1996.
- [85] R. W. Longman, "Iterative Learning Control and Repetitive Control for Engineering Practice," *International journal of control*, vol. 73, no. 10, pp. 930-954, 2000.
- [86] Z. Bien and K. M. Huh, "Higher-Order Iterative Learning Control Algorithm," in *IEE Proceedings D (Control Theory and Applications)*, 1989, vol. 136, no. 3: IET, pp. 105-112.
- [87] P. B. Goldsmith, "The Fallacy of Causal Iterative Learning Control," in *Proceedings of the 40th IEEE Conference on Decision and Control (Cat. No. 01CH37228)*, 2001, vol. 5: IEEE, pp. 4475-4480.
- [88] P. B. Goldsmith, "On the Equivalence of Causal Lti Iterative Learning Control and Feedback Control," *Automatica*, vol. 38, no. 4, pp. 703-708, 2002.
- [89] D. H. Owens and E. Rogers, "Comments On/on the Equivalence of Causal Lti Iterative Learning Control and Feedback Control," *Automatica*, vol. 40, no. 5, pp. 895-898, 2004.
- [90] D. De Roover and O. H. Bosgra, "Synthesis of Robust Multivariable Iterative Learning Controllers with Application to a Wafer Stage Motion System," *international Journal of Control*, vol. 73, no. 10, pp. 968-979, 2000.

- [91] Y. Chen and K. L. Moore, "An Optimal Design of Pd-Type Iterative Learning Control with Monotonic Convergence," in *Proceedings of the IEEE International Symposium on Intelligent Control*, 2002: IEEE, pp. 55-60.
- [92] M. Norrlöf and S. Gunnarsson, "Time and Frequency Domain Convergence Properties in Iterative Learning Control," *International Journal of Control*, vol. 75, no. 14, pp. 1114-1126, 2002.
- [93] J. H. Lee, K. S. Lee, and W. C. Kim, "Model-Based Iterative Learning Control with a Quadratic Criterion for Time-Varying Linear Systems," *Automatica*, vol. 36, no. 5, pp. 641-657, 2000.
- [94] K. L. Moore, Y. Chen, and V. Bahl, "Monotonically Convergent Iterative Learning Control for Linear Discrete-Time Systems," *Automatica*, vol. 41, no. 9, pp. 1529-1537, 2005.
- [95] H.-S. Lee and Z. Bien, "A Note on Convergence Property of Iterative Learning Controller with Respect to Sup Norm," *Automatica*, vol. 33, no. 8, pp. 1591-1593, 1997.
- [96] J.-X. Xu and Y. Tan, *Linear and Nonlinear Iterative Learning Control*. Springer, 2003.
- [97] Y. Chen and C. Wen, *Iterative Learning Control: Convergence, Robustness and Applications*. Springer London, 1999.
- [98] Y. Chen, C. Wen, and M. Sun, "A Robust High-Order P-Type Iterative Learning Controller Using Current Iteration Tracking Error," *International Journal of Control*, vol. 68, no. 2, pp. 331-342, 1997.
- [99] Y. Chen, Z. Gong, and C. Wen, "Analysis of a High-Order Iterative Learning Control Algorithm for Uncertain Nonlinear Systems with State Delays," *Automatica*, vol. 34, no. 3, pp. 345-353, 1998.
- [100] D. H. Owens and K. Feng, "Parameter Optimization in Iterative Learning Control," *International Journal of Control*, vol. 76, no. 11, pp. 1059-1069, 2003.
- [101] M. Q. Phan, R. W. Longman, and K. L. Morre, "Unified Formulation of Linear Iterative Learning Control," *Spaceflight mechanics 2000*, pp. 93-111, 2000.
- [102] H. Elci, R. W. Longman, M. Q. Phan, J.-N. Juang, and R. Ugoletti, "Simple Learning Control Made Practical by Zero-Phase Filtering: Applications to Robotics," *IEEE Transactions on Circuits and Systems I: Fundamental Theory and Applications*, vol. 49, no. 6, pp. 753-767, 2002.
- [103] T. Kavli, "Frequency Domain Synthesis of Trajectory Learning Controllers for Robot Manipulators," *Journal of Robotic Systems*, vol. 9, no. 5, pp. 663-680, 1992.
- [104] D.-I. Kim and S. Kim, "An Iterative Learning Control Method with Application for Cnc Machine Tools," *IEEE Transactions on Industry Applications*, vol. 32, no. 1, pp. 66-72, 1996.
- [105] D. Gorinevsky, "Loop Shaping for Iterative Control of Batch Processes," *IEEE Control Systems Magazine*, vol. 22, no. 6, pp. 55-65, 2002.
- [106] Y. Tan and J.-X. Xu, "Learning Based Nonlinear Internal Model Control," in *Proceedings of the 2003 American Control Conference, 2003.*, 2003, vol. 4: IEEE, pp. 3009-3013.
- [107] D. Meng, "Convergence Conditions for Solving Robust Iterative Learning Control Problems under Nonrepetitive Model Uncertainties," *IEEE transactions on neural networks and learning systems*, vol. 30, no. 6, pp. 1908-1919, 2018.
- [108] D. Meng and K. L. Moore, "Robust Iterative Learning Control for Nonrepetitive Uncertain Systems," *IEEE Transactions on Automatic Control*, vol. 62, no. 2, pp. 907-913, 2016.
- [109] Y. Chen, C. Wen, Z. Gong, and M. Sun, "An Iterative Learning Controller with Initial State Learning," *IEEE Transactions on Automatic Control*, vol. 44, no. 2, pp. 371-376, 1999.
- [110] F. M. White, *Fluid Mechanics*, 7th ed. McGraw-Hill, 2011.
- [111] Y. A. Çengel, *Heat and Mass Transfer – a Practical Approach*, 3rd ed. McGraw-Hill, 2007.
- [112] I. L. Krivts and G. V. Krejnin, *Pneumatic Actuating Systems for Automatic Equipment: Structure and Design*. Crc Press, 2016.

